

NACA RM E53G16

**NACA**

TECH LIBRARY KAFB, NM  
0143248

# RESEARCH MEMORANDUM

EVALUATION OF EFFECTS OF RANDOM PERMEABILITY VARIATIONS  
ON TRANSPIRATION-COOLED SURFACES

By Jack B. Esgar and Hadley T. Richards

Lewis Flight Propulsion Laboratory  
Cleveland, Ohio

Classification cancelled (or changed to) Unclassified  
By authority of NASA Tech Rep Announcement # 118  
(OFFICER AUTHORIZED TO CHANGE)  
By 16 Aug 57  
NAME AND AK  
GRADE OF OFFICER MAKING CHANGE  
DATE 31 Mar 61

**NATIONAL ADVISORY COMMITTEE  
FOR AERONAUTICS**

WASHINGTON  
November 30, 1953

RECEIPT SIGNATURE  
RECEIVED



0143248

NACA RM E53G16

## NATIONAL ADVISORY COMMITTEE FOR AERONAUTICS

RESEARCH MEMORANDUMEVALUATION OF EFFECTS OF RANDOM PERMEABILITY VARIATIONS ON  
TRANSPIRATION-COOLED SURFACES

By Jack B. Esgar and Hadley T. Richards

## SUMMARY

Fabrication techniques utilized for the manufacture of porous, transpiration-cooled surfaces may result in random permeability variations that could seriously affect the efficiency of this means of cooling surfaces that must be in contact with high-temperature gas streams. Therefore, an analytical investigation was conducted to evaluate the effects of permeability variations on surface temperatures and coolant flows for ranges of temperature and Reynolds number that are of particular interest for gas-turbine blades. In addition, experimental studies under static conditions were made on small orifices and on an experimental, sintered, porous turbine blade utilizing orifices at the base for partially metering the cooling-air flow. Measurements of flow through the small orifices and through the blade were used for partial verification of the analytical investigation, which showed that considerable care is required to minimize random permeability variations in gas-turbine blades. In order to keep blade temperature variations to less than  $\pm 100^{\circ}\text{F}$ , a random permeability variation of not over  $\pm 6$  percent is required for a turbine-inlet gas temperature of  $2500^{\circ}\text{F}$ , and not over  $\pm 10$  percent for a turbine-inlet temperature of  $1600^{\circ}\text{F}$ . Operation at high gas Reynolds numbers or low permeabilities will permit somewhat greater local permeability variations. The use of orifices in series with the porous surface is of considerable advantage in improving transpiration-cooling efficiency at off-design engine conditions, and it simplifies blade manufacture; but the orifices do not reduce temperature variations due to variations in permeability. In fact, in some cases the temperature variations are higher than for the case in which the porous wall does not have an orifice in series.

The fabrication method used on the experimental blade provided a means whereby a thin, porous, sintered shell can be attached to a central strut; however, the attachment method must be investigated under conditions of high rotational speed, and the random permeability variations in the blade were greater than could be tolerated in a turbojet engine. From the results of this and other investigations, it was possible to provide recommended design features for transpiration-cooled turbine blades.

## INTRODUCTION

Transpiration cooling is the most effective air-cooling method known at present for surfaces that must be in contact with high-temperature gas streams (ref. 1); however, random variations in wall permeability may cause surface-temperature or coolant-flow variations that will seriously affect the efficiency of this means of cooling. Therefore, an investigation was conducted at the NACA Lewis laboratory to evaluate the effects of random permeability variations on surface temperatures and coolant flows for transpiration-cooled surfaces for ranges of temperature and Reynolds number that are of particular interest for gas-turbine blades.

There is a high pressure gradient on the outside surface of gas-turbine blades, so that at some locations on the blade the pressure level may be on the order of only one-half the pressure level at the blade leading edge. Since in transpiration cooling the local coolant flow is a function of the pressure difference between the cooling-supply pressure (which must be higher than the pressure at the leading edge) and the local pressure on the outside surface of the blade, a method of control is required in order to obtain the proper coolant-flow distribution over the blade surface. Two methods that have been considered are: (1) varying the permeability around the periphery of the porous shell, or (2) dividing the blade coolant passage into compartments and providing an orifice at the base of each compartment so that the orifice is in series with the porous shell; the orifice then provides part of the pressure drop between the coolant-supply pressure and the local pressure on the outside surface of the blade (ref. 2).

It is shown in reference 2 that, for ordinary transpiration-cooled turbine blades that do not utilize orifices in the blade base for partially metering the cooling air, relatively small variations in permeability result in substantial changes in cooling-air flow requirements for turbine blades that must have adequate cooling over a considerable range of flight altitude. Reference 2 also indicates that the use of orifices at the base of turbine blades makes transpiration-cooled turbine blades cool more uniformly over a wide range of altitude and greatly simplifies problems in the fabrication of blades. It has not been determined in previous investigations, however, to what extent variations in specified permeability can be tolerated without resulting in excessive variations in cooled surface temperature or resulting in exorbitant increases in cooling-air requirements.

In order to obtain a better understanding of permissible permeability variations, an analytical investigation was conducted to determine the effect of random permeability variations on coolant-flow rates

and porous surface temperatures for ranges of temperature, pressure, and Reynolds number that would be of interest for gas-turbine blades designed for flight altitudes from sea level to 50,000 feet and compressor pressure ratios from about 4 to 10. Ranges of permeability, designated as  $12K'/\tau$ , from  $16 \times 10^{-9}$  to  $72 \times 10^{-9}$  inch were considered. (The permeability term will be explained later.) Calculations were made for orifices in the blade base that would result in orifice pressure drops from zero to approximately nine-tenths of the pressure drop from the coolant-supply pressure to the pressure on the outside surface of the porous wall. Wall temperatures of  $1000^{\circ}$  and  $1500^{\circ}$  F and turbine-inlet gas temperatures of  $1600^{\circ}$  and  $2500^{\circ}$  F were considered.

In conjunction with the analytical investigation, experimental studies were made on small orifices and on an experimental, porous, sintered turbine blade utilizing orifices at the base for partially metering the cooling-air flow. Measurements of flow through the small orifices and through the blade were used for partial verification of the analytical procedure. From the measured permeabilities on the blade, it was possible to evaluate variations in local flow rates and in wall temperatures that could be expected in actual practice at the present stage of development in transpiration-cooled turbine blades. The experimental porous blade used for this part of the investigation was fabricated by the Federal-Mogul Corporation.

#### APPARATUS AND EXPERIMENTAL PROCEDURE

Cooling-air flow rates were measured through small orifices, through porous metal walls of a turbine blade, and through the orifices and the porous metal wall in series. The data were obtained in order to determine the accuracy of analytical methods of flow correlation, and the permeability variations over the surface of the experimental, sintered, porous turbine blade fabricated for static tests.

##### Small-Orifice Calibration

The use of orifices at the base of turbine blades is beneficial if the flow through the orifices is governed by the laws of a flow nozzle, according to reference 2. Therefore, calibration runs were made to determine whether flow through orifices follows the laws governing flow through a flow nozzle when the orifice diameter is small and the plate thickness relative to standard flat-plate orifice practice is large.

For these tests, orifices with diameters of 0.020, 0.040, and 0.060 inch were drilled in plates 0.047 inch thick. A 0.040-inch-diameter orifice was also tested with the upstream face chamfered in an effort to



duplicate more nearly a flow-nozzle configuration. The orifice plates were made in the form of disks and were mounted in an apparatus similar to that used in references 3 and 4 for flow-testing porous metal disks. The air passing through the orifices was not heated in the investigation presented herein. In all cases a single orifice was located in the center of a 2-inch-diameter disk. The flow rate through the orifice was measured by a positive-displacement meter, and the pressure upstream of the orifice by a static tap. In all cases the pressure downstream of the orifice was the barometric pressure. The calibrations were made at barometer readings from 2040 to 2074 pounds per square foot and at air temperatures from 72° to 85° F.

#### Porous-Blade Calibration

Apparatus. - Photographs of the sintered, porous turbine blade used in static tests in this investigation are shown in figure 1. The blade chord is approximately 2 inches and the span is 5 inches. The blade shell is made of porous copper-nickel-tin (bronze) of approximately 0.035-inch thickness and is attached to the non-porous low-alloy steel strut. A bronze porous shell would not be suitable for use in a turbo-jet engine, however, because the shell cannot withstand temperatures much in excess of 600° F. A shell temperature of about 1000° F is considered about minimum for engine application; therefore, this blade would not be suitable for heat-transfer tests. The blade was made to study fabrication methods and techniques of permeability control for the manufacturing process used. Additional research will be required on similar blades to determine whether the shell attachment method will be suitable at high rotational speeds.

The fabrication of the blade is discussed in reference 5. Briefly, the process was as follows: The strut was machined from a low-alloy steel, and then the cooling-air passages between adjacent fins were packed with a mixture of powdered graphite and a liquid containing 50 percent collodion and 50 percent ether. The strut was next placed inside a graphite mold, and spherical bronze powder was vibrated into place around the strut to form the 0.035-inch-thick wall. The blade was sintered inside the mold for 50 minutes at 1775° F, a temperature that lies between the liquidus and solidus temperatures of the metal powder. After sintering, the graphite in the cooling-air passages was cleaned out with an air blast. This fabrication method makes use of the sintering temperature and the particle size of the porous metal to control the permeability of the porous shell. The final control of the permeability of the blade is accomplished by the incorporation of an orifice plate at the blade base that provides an orifice for each cooling-air passage. The orifice plate is shown detached from the blade in figure 1(a) and assembled on the blade in figure 1(b). A blank plate is attached at the blade tip, so that all cooling air must flow through the porous shell of the blade.

In the fabrication of this blade, an attempt was made to produce specified apparent permeabilities around the perimeter of the turbine blade. (Apparent permeability is defined as a permeability measurement resulting from an orifice in series with a porous wall.) In an effort to produce a blade of approximate permeabilities that would be on the order required for immediate incorporation in an experimental test engine, apparent permeabilities were specified that would be suitable for an engine having a turbine-inlet temperature of 1600° F, a compressor pressure ratio of 4, and an altitude range from sea level to 50,000 feet. In order to simplify fabrication, an accurate permeability variation was not specified; instead, approximate permeabilities were specified for the leading edge, suction surface, and pressure surface, as follows:

Position	Apparent permeability, $(12K'/\tau)_{ap}$ , in.
Leading edge	$14.2 \times 10^{-9}$
Suction surface	$8.7 \times 10^{-9}$
Pressure surface	$10.4 \times 10^{-9}$

The orifice sizes for the blade were determined experimentally to compensate for variations in the shell permeability that resulted from the manufacturing procedure used and to obtain the specified apparent permeability that will result in approximately the proper average coolant-flow rates around the blade periphery. A recommended procedure for selecting wall permeabilities and orifice sizes is discussed under CALCULATION PROCEDURE. For experimentally flow-checking, the blade was installed in a holder as shown in figure 1(c) and mounted in an apparatus similar to that described in reference 4.

Experimental procedure. - By use of a probe in the manner described in reference 4, the local flow rates were measured around the blade periphery at three spanwise positions (root, midspan, and tip) for a coolant-supply pressure that permits conversion of the measured flow rates to a measure of permeability indicated by  $12K'/\tau$ . (The equation for this conversion is given in the CALCULATION PROCEDURE.) These measurements were made both with and without the orifice plate at the blade root and gave an indication of the permeability distribution over the surface of the blade with and without orifices. There was some disagreement between coolant-flow rates measured by the manufacturer of the experimental blade and the coolant-flow rates measured by the NACA. The NACA apparatus was then recalibrated, and the original NACA measurements appear to be reasonably accurate.

In addition to the coolant-flow surveys made around the blade periphery, more complete surveys were made along the span at a single chordwise position. These surveys were made for a range of pressure drops to determine the effect, if any, of pressure drop along the coolant passage formed between adjacent fins on the strut and to determine whether the flow through an orifice and a porous wall in series behaves in the manner expected from analytical considerations.

### CALCULATION PROCEDURE

In order to generalize the results of this investigation as much as possible, calculations are made for no particular turbine or engine configuration, but are generalized to cover ranges of permeability, Reynolds number, orifice size, temperature, and pressure that might be expected in the reasonable future for turbine rotors operating in engines with compressor pressure ratios up to about 10. The calculation procedure is based upon the assumption that, for a given set of conditions and a specified permeability, the transpiration-cooled surface is cooled to some specified temperature. For these given conditions, changes in coolant-flow rate and surface temperature are then calculated for random variations in permeability. The procedure for making these calculations and the method used for specifying wall permeability and orifice size are outlined in the following paragraphs.

#### Method of Specifying Permeability

Analytical calculations. - As shown in references 3 and 4, the flow through a porous surface can be correlated by a plot of  $\frac{\mu_0^{2T_0}}{\mu_{a,B}^2} \frac{p_a^2 - p_g^2}{\tau}$

as ordinate against  $\frac{\mu_0}{\mu_{a,B}} \rho_a v_a$ . (Symbols are defined in the appendix.)

If the data are plotted on logarithmic coordinates, as are the figures in reference 3, the curves for any two permeable materials have practically uniform vertical displacement. It should be possible, therefore, to use a single curve that would generalize all permeability data by plotting

$\frac{\mu_0^{2T_0}}{\mu_{a,B}^2} (p_a^2 - p_g^2) \beta$  against  $\frac{\mu_0}{\mu_{a,B}} \rho_a v_a$ , where  $\beta = C/\tau$ . The value of  $\beta$

(or the constant  $C$ ), which is a function of the material permeability, can be evaluated in the following manner:

- (1) Establish an experimental general curve similar to figure 2 for a representative material of a given permeability and let  $C = 1.0$ .
- (2) For a material of any other permeability, determine experimentally the value of  $\beta$  which will result in a permeability correlation curve that will be coincident with the general curve established in step (1).

From the method outlined herein, any value of permeability  $K'/\tau$  has a corresponding value of  $\beta$ . From reference 2 the value of  $K'/\tau$  is given as

$$\frac{K'}{\tau} = \frac{2RT_0\mu_0(\rho_a v_a)\Omega}{(p_a - h_B)^2 - p_g^2} \quad (1)$$

where the value of  $(\rho_a v_a)\Omega$  is specified for NACA standard sea-level temperature and for  $p_a - h_B = 3556$  pounds per square foot and  $p_g = 2116$  pounds per square foot. Substituting the appropriate values in equation (1) results in

$$\frac{12K'}{\tau} = 30.6(\rho_a v_a)\Omega \times 10^{-9} \text{ in.} \quad (2)$$

The factor 12 in equation (2) is a conversion from feet to inches, because the permeability coefficient  $K$  is normally specified in the literature in square inches. The permeability coefficient  $K'$  corresponds to the conditions stated for equations (1) and (2); and, as explained in reference 2, it differs from the permeability coefficient  $K$ , which is obtained by extrapolation of experimental data to the condition where  $\rho_a v_a = 0$ .

When equation (2) is used without an orifice ( $h_B = 0$ ), the term  $12K'/\tau$  is called the permeability. The same equation is used with an orifice in series with a porous wall ( $h_B \neq 0$ ), but the resulting value obtained from the equation is the apparent permeability and is designated  $(12K'/\tau)_{ap}$ .

Experimental calculations. - In the evaluation of the permeability  $12K'/\tau$  from equation (2) and a single measured value of the flow  $\rho_a v_a$  as discussed in APPARATUS AND EXPERIMENTAL PROCEDURE, it is necessary to obtain the flow rate at a pressure level and pressure drop that will result in correct values in equation (1). The procedure for determining the desired pressure levels is as follows:

(1) If a permeability correlation plot of  $\frac{\mu_0^{2T_0}}{\mu_{a,B}^{2T_{a,B}}} \frac{p_a^2 - p_g^2}{\tau}$  against

$\frac{\mu_0}{\mu_{a,B}} \rho_a v_a$  is available, the value of  $(\rho_a v_a)_{\Omega}$  is read from the curve for the case where  $\mu_0^{2T_0}/\mu_{a,B}^{2T_{a,B}}$  and  $\mu_0/\mu_{a,B}$  are numerically equal to 1.0 and  $p_a^2 - p_g^2 = 3556^2 - 2116^2 = 8.168 \times 10^6$  lb<sup>2</sup>/ft<sup>4</sup>. For cases in which it is desirable to measure the flow rate directly without obtaining data sufficient for plotting a correlation curve, and in which the cooling-air temperature is different from 518.4° R, it is necessary for the conditions of the test that  $\frac{\mu_0^{2T_0}}{\mu_{a,B}^{2T_{a,B}}} (p_a^2 - p_g^2) = 8.168 \times 10^6$  lb<sup>2</sup>/ft<sup>4</sup>. If the cooling air is discharging to atmospheric pressure, the coolant-supply pressure should be

$$p_a = \sqrt{\frac{8.168 \times 10^6}{\frac{\mu_0^{2T_0}}{\mu_{a,B}^{2T_{a,B}}}} + p_g^2} \quad (3)$$

(2) The flow rate  $(\rho_a v_a)_{\Omega}$  for use in equation (2) is then obtained from

$$(\rho_a v_a)_{\Omega} = \frac{\mu_0}{\mu_{a,B}} \rho_a v_a \quad (4)$$

where  $\rho_a v_a$  is the experimentally measured flow rate. The values of  $\mu_0^{2T_0}/\mu_{a,B}^{2T_{a,B}}$  and  $\mu_0/\mu_{a,B}$  for the cooling-air temperature  $T_{a,B}$  can be obtained from table I of reference 3.

#### Method of Specifying Orifice Size

The orifices are used at the base of transpiration-cooled turbine blades so that part of the pressure drop between the coolant-supply pressure and the pressure on the gas side of the porous wall will be taken through the orifice. The smaller the orifice for a given porous-wall

surface area, the greater will be the pressure drop across the orifice. In these calculations, however, it is desired to generalize the results as much as possible; therefore, instead of specifying orifice size, a factor will be introduced in the orifice equation that will determine the ratio of the pressure drop through the orifice to the over-all pressure drop from the coolant supply to the discharge on the gas side of the porous wall for a standard set of conditions. The procedure will be as follows: The subsonic flow through an orifice in the form of a flow nozzle can be expressed as

$$\rho_a v_a = \frac{A_n B}{A_a} \sqrt{\frac{2g}{R} \frac{h_B (p_a - h_B)}{T_{a,n}}} \quad (5)$$

where

$p_a$  coolant-supply pressure ahead of orifice

$p_a - h_B$  local coolant-supply pressure inside turbine blade (pressure after orifice)

$h_B$  pressure drop across orifice

When the subscript  $\Omega$  is used to designate a standard set of flow conditions for specifying the orifice size, equation (5) can be written

$$\frac{A_n B}{A_a} = \frac{(\rho_a v_a)_{\Omega}}{\sqrt{\frac{2g}{R} \frac{h_{B,\Omega} (p_{a,\Omega} - h_{B,\Omega})}{T_0}}} \quad (6)$$

where the value of  $(\rho_a v_a)_{\Omega}$  is the same value used for specifying the permeability in equation (2), and  $p_{a,\Omega} = 3556$  pounds per square foot. The value of  $h_{B,\Omega}$  will then determine the orifice size. The larger the value of  $h_{B,\Omega}$  the greater will be the proportion of the total cooling-air pressure drop through the orifice, and the smaller will be the proportion of the total pressure drop through the porous wall. The numerical values of  $h_{B,\Omega}$  will normally be less than 1500 pounds per square foot. Except for very high values of  $h_{B,\Omega}$ , the ratio of the pressure drop through the orifice to the over-all pressure drop from the coolant-supply pressure to the discharge pressure on the gas side of the blade will be approximately equal to  $h_{B,\Omega}/1440$ .

CONFIDENTIAL

For supercritical pressure drops across a flow nozzle ( $h_B \geq 0.472p_a$ ), the flow equation can be obtained from reference 6 in the exact form (for  $\gamma = 1.4$ ):

$$\rho_a v_a = \frac{A_{nB}}{A_a} \frac{0.484 p_a}{\sqrt{\frac{T_{a,n} R}{2g}}} \quad (5a)$$

### Calculation of Pressure Drops for Orifices in Series

#### with Porous Walls

By use of a correlation plot of flow through porous surfaces, such as figure 2, and the orifice flow equation (5), it is possible to calculate the pressure drop through the orifice and porous surface for specified coolant-flow rates and orifice sizes.

For specified values of permeability (and thus  $\beta$ ), orifice size, coolant-supply pressure  $p_a$ , and coolant flow  $\rho_a v_a$ , the discharge pressure  $p_g$  can be calculated as follows:

- (1) For a given or required value of  $\rho_a v_a$ , calculate  $h_B$  by use of equation (5) written in the form

$$h_B = \frac{p_a}{2} - \sqrt{\frac{p_a^2}{4} - \frac{RT_{a,n}}{2g} \left( \frac{\rho_a v_a}{A_{nB}/A_a} \right)^2}$$

(The locations of pressures  $p_a$ ,  $p_a - h_B$ , and  $p_g$  are shown in fig. 3.)

- (2) Using the values of  $h_B$  and  $\rho_a v_a$  from the above step and using the porous metal temperature for evaluating  $\mu_0/\mu_{a,B}$  and

$\mu_0^{2T_0}/\mu_{a,B}^{2T_{a,B}}$ , read  $\frac{\mu_0^{2T_0}}{\mu_{a,B}^{2T_{a,B}}} \left[ (p_a - h_B)^2 - p_g^2 \right] \beta$  from a correla-

tion curve of the porous material, such as shown in figure 2, and then calculate the resulting discharge pressure  $p_g$ . The values of  $\mu_0/\mu_{a,B}$  and  $\mu_0^{2T_0}/\mu_{a,B}^{2T_{a,B}}$  can be obtained from table I of reference 3.



If the discharge pressure  $p_g$  is known instead of the coolant-supply pressure  $p_a$ , iteration will be required to obtain  $p_a$ . It will be necessary to assume values of  $p_a$  until, with the above procedure, the calculated value of  $p_g$  agrees with the known (or specified) value. If this procedure results in  $h_B \geq 0.472p_a$ , then  $p_a$  should be calculated from equation (5a).

### Calculation of Required Flow Rates for Specified

#### Wall Temperatures

In reference 7, Friedman developed an equation for determination of wall temperatures for turbulent-flow transpiration cooling. Friedman's equation is

$$\frac{T_B - T_a}{T_{g,e} - T_a} = \frac{r}{e^{r\varphi} + r - 1} \quad (7)$$

In reference 8, the values of  $\varphi$  and  $r$  are given as

$$\varphi = \frac{Re_g^{1/5} Pr_g^{2/3}}{0.0296} \frac{\rho_a v_a}{\rho_g \bar{V}_g} \quad (8)$$

and

$$r = \frac{2.11}{Re_g^{0.1}} \quad (9)$$

In reference 2, the equation for  $\varphi$  (eq. (8)) was altered by using a Reynolds number where the density and viscosity were based on the blade wall temperature, because outside heat-transfer coefficient data can usually be better correlated in this manner for a large range of  $T_g/T_B$ . Since the publication of reference 2, however, experimental data have become available on a transpiration-cooled combustion-chamber wall of an afterburner (ref. 9) where the temperature ratio  $T_g/T_B$  was as high as 6. In an effort to determine whether the Reynolds number in equation (8) should have the density and viscosity based on wall temperature or stream temperature, calculations were made to determine whether the experimental

results in reference 9 could be predicted analytically by means of equation (7). It was found that, for high temperature ratios, basing the density and viscosity on wall temperature (as was done in ref. 2) resulted in calculated wall temperatures considerably in excess of those measured experimentally. If the density and Reynolds number were based on the gas temperature, however, very good agreement was obtained between analytical and experimental results. For example, for a gas temperature of 2500° F and a cooling-air temperature of 200° F, the maximum difference between analytically predicted and average experimentally measured temperatures was less than 50° F for a wide range of cooling-air flow. For this reason, the density and viscosity in the Reynolds number will be based on gas temperature in this report. It should be noted that the characteristic dimension in the Reynolds number was taken as the diameter for the afterburner, and the effects of radiant heat transfer were neglected. For turbine blades, the characteristic dimension is taken as the distance from the blade leading edge to the location on the blade where the temperature is being calculated.

By combining equations (8) and (9) and noting that

$$\rho_g v_g = \frac{Re_g g \mu_g}{x}$$

the following expression is obtained:

$$r\phi = \frac{71.3(\rho_a v_a) Pr_g^{2/3}}{Re_g^{0.9}} \frac{x}{g \mu_g} \quad (10)$$

Equations (7) and (10) can be combined and solved for  $\rho_a v_a$ :

$$\rho_a v_a = \frac{Re_g^{0.9} \ln \left( 1 - r + \frac{r}{\frac{T_B - T_a}{T_{g,e} - T_a}} \right)}{71.3 Pr_g^{2/3} \frac{x}{g \mu_g}} \quad (11)$$

Calculations were not made for laminar-flow transpiration cooling. At this time there is no experimental evidence available concerning the extent of the laminar boundary layer on transpiration-cooled gas-turbine blades. In reference 10, however, it is shown that for a flat plate the boundary layer is almost certain to be turbulent for the quantities of

coolant flow that are required for turbine cooling. Gas-turbine blades differ from a flat plate in that there is a pressure gradient which will have a stabilizing influence in helping to extend the laminar boundary layer farther from the leading edge than would be obtained on a flat plate. However, it is expected that for many gas-turbine blades only a small portion of the boundary layer near the blade leading edge will be laminar. Furthermore these transpiration-cooling calculations are made for the purpose of indicating the approximate effect of random permeability variations on coolant flow and wall temperature. These effects are evaluated by a generalized method, and it is believed that consideration of laminar-flow transpiration cooling for this specific purpose would not significantly affect the conclusions to be drawn.

#### Calculation of Temperature Variations Due to Random

##### Permeability Variations

In order to obtain a specified wall temperature for given values of gas and coolant temperature and gas Reynolds number, a certain coolant-flow rate is required that is independent of permeability, pressure level, or pressure drop through the porous wall. All calculations in this report were made for specified coolant supply pressures. For a specified coolant-supply pressure  $p_a$  and a specified permeability  $(12K'/\tau)_{std}$ , there is a coolant-discharge pressure that will result in the required coolant-flow rate. If there are variations in permeability over a porous surface, local coolant-flow rates will also vary over the surface. These variations will in turn cause the local surface temperatures of a transpiration-cooled surface to vary. The amount of flow through a porous surface is also influenced by the surface temperature, so that for transpiration cooling the permeability variations, local coolant-flow rates, and local surface temperatures are all interdependent. Methods of calculating the effects of random permeability variations on local coolant-flow rates and on local surface temperatures for the cases with and without orifices in series with the porous wall are discussed individually.

No orifices in series with porous wall. - The following procedure is used for calculating the effects of random permeability variations on local coolant-flow rates and surface temperatures for a set value of coolant-supply pressure and a discharge pressure determined for specified temperatures and permeability:

- (1) The coolant flow required to obtain a specified wall temperature is calculated by means of equation (11).
- (2) For a specified permeability  $(12K'/\tau)_{std}$ , the factor  $\beta$  is calculated as previously discussed.

- (3) The value of  $p_g$  is calculated by using the permeability correlation curve in figure 2 with  $h_B = 0$ , the specified wall temperature  $T_B$  for evaluating the quantities  $\mu_O^{2T_O}/\mu_{a,B}^{2T_{a,B}}$  and  $\mu_O/\mu_{a,B}$ , a specified value of  $p_a$ , and values of  $\rho_a v_a$  and  $\beta$  from steps (1) and (2).
- (4) Iteration will be required to obtain the temperature that will result from a random variation in permeability. For a value of permeability different from the specified value used in steps (2) and (3), the value of  $\beta$  will be different. A value of porous-surface temperature must be assumed. With an assumed surface temperature  $T_B$  used for evaluating the quantities  $\mu_O^{2T_O}/\mu_{a,B}^{2T_{a,B}}$  and  $\mu_O/\mu_{a,B}$ , with the new value of  $\beta$ , and with the value of  $p_g$  from step (3), a new value of  $\rho_a v_a$  is obtained from figure 2 (letting  $h_B = 0$ ) for the new permeability  $12K'/\tau$ .
- (5) The resulting porous-wall temperature is calculated from equations (7), (9), and (10), and the coolant-flow rate  $\rho_a v_a$  from step (4). If this calculated value of wall temperature does not agree with the assumed value in step (4), iteration is required until agreement is reached.

With orifices in series with porous wall. - With an orifice of a specified size in series with a porous wall, the pressure drop across the orifice is a function of the pressure level, the coolant temperature, and the flow rate. For specified coolant-supply and coolant-discharge pressures, the orifice pressure drop  $h_B$  is therefore a function of the average permeability of the porous wall. Local variations in coolant flow and wall temperature due to local variations in permeability will be influenced by the pressure after the orifice  $p_a - h_B$  and the coolant-discharge pressure  $p_g$ . It is necessary, therefore, to have a knowledge of the average permeability of the porous surface being fed by an orifice before it is possible to calculate the effect of local permeability variations on coolant-flow rates and wall temperatures. If the average permeability  $(12K'/\tau)_{av}$  is known, the flow and temperature variations can be calculated as follows:

- (1) The coolant flow required to obtain a specified wall temperature and the factor  $\beta$  for the specified permeability are calculated as described in steps (1) and (2) for the case with no orifices.

- (2) The average permeability  $(12K'/\tau)_{av}$  is assumed the same as the specified permeability  $(12K'/\tau)_{std}$ , and a specified value of  $p_a$  and values of  $\rho_a v_a$  and  $\beta$  from step (1) are used to calculate  $p_g$  by the procedure discussed in the section Calculation of Pressure Drops for Orifices in Series with Porous Walls, where the cooling-air temperature  $T_{a,n}$  is used in equation (5) and the specified wall temperature  $T_B$  equal to  $T_{a,B}$  is used for evaluating the quantities  $\mu_0^2 T_0 / \mu_{a,B}^2 T_{a,B}$  and  $\mu_0 / \mu_{a,B}$ . The value of  $A_n B / A_a$  is obtained (for eq. (5)) from equation (6) for a specified value of  $h_{B,\Omega, std}$  or from a specified orifice area  $A_n$  and porous-surface area  $A_a$ .
- (3) With figure 2 and the values of  $\rho_a v_a$ ,  $\beta$ ,  $T_B$ , and  $p_g$  from step (2),  $p_a - h_B$  is calculated, which is the supply pressure to the porous wall of variable permeability.
- (4) From figure 2 and a procedure similar to steps (4) and (5) for the procedure with no orifices, the local temperatures are obtained by iteration for the value of  $p_a - h_B$  from step (3) and the value of  $p_g$  from step (2) of this procedure.
- (5) If the average permeability  $(12K'/\tau)_{av}$  is not equal to the specified permeability  $(12K'/\tau)_{std}$ , the procedure outlined herein will not result in the attainment of the specified temperature for the specified permeability. Double iteration would then be required to obtain the pressure  $p_g$  which would result in a coolant-flow rate that would cause a specified temperature to be obtained at the location on the surface having the specified permeability.

The calculation procedures described in this section were used for this analysis where it was convenient to specify the coolant-supply pressure in order to generalize the results. For a gas-turbine engine, the coolant-discharge pressure  $p_g$  is set by the engine cycle and the velocity distribution over the turbine blades and therefore cannot be used as an independent variable. For a specific engine calculation, it would, therefore, be necessary to alter slightly the procedure given herein and to solve for the required coolant-supply pressure  $p_a$  instead of for the discharge pressure  $p_g$ .

### Assumed Conditions for Calculations

For the analytical results of this report, the following conditions were assumed:

- (1) The Prandtl number had a constant value of 0.66.
- (2) All calculations were made for a location  $x$ , 1 inch from the leading edge of the porous surface. This would be a typical distance for the approximate midchord section of a turbine rotor blade and probably would be in a turbulent-boundary-layer region on the blade.
- (3) Cooling-air temperatures at the blade root of  $340^{\circ}$  and  $740^{\circ}$  F were assumed.
- (4) Values of gas viscosity  $\mu_g$  were assumed to be the same as values given for air in references 11 or 3.
- (5) Calculations were made for turbine-inlet temperatures of  $1600^{\circ}$  and  $2500^{\circ}$  F, which correspond to rotor blade effective gas temperatures  $T_{g,e}$  of  $1334^{\circ}$  and  $2265^{\circ}$  F, respectively, for the configuration assumed in reference 2.
- (6) Calculations were made for gas Reynolds numbers of  $2 \times 10^4$ ,  $2 \times 10^5$ , and  $2 \times 10^6$  and coolant-supply pressures of 1350 and 9600 pounds per square foot. These ranges of Reynolds number and coolant-supply pressure cover the ranges to be expected for turbine rotor blades in engines operating from sea level to 50,000 feet altitude for engine compressor pressure ratios from 4 to 10.
- (7) Calculations were made to determine the effect of random variations in porous-wall permeability up to  $\pm 20$  percent for specified permeabilities  $(12K'/\tau)_{std}$  of  $20 \times 10^{-9}$ ,  $40 \times 10^{-9}$ , and  $72 \times 10^{-9}$  inch.
- (8) Specified blade temperatures were  $1000^{\circ}$  F for turbine-inlet gas temperatures of  $1600^{\circ}$  and  $2500^{\circ}$  F, and also  $1500^{\circ}$  F for a gas temperature of  $2500^{\circ}$  F.
- (9) Orifice sizes were assumed that would result in an orifice pressure drop of from zero to approximately nine-tenths of the pressure drop from the coolant-supply pressure to the pressure on the outside surface of the blade wall.
- (10) The relation between flow and pressure drop through the porous surfaces was obtained from figures 2 and 4. Figure 2 gives the correlation for flow for all permeabilities for which the value of the term  $\beta$  may be obtained from figure 4. The experimental data for figure 2 were obtained from reference 3, and the values of  $\beta$  were calculated by the method previously discussed.

## RESULTS AND DISCUSSION

## Small-Orifice Calibrations

The results of calibrations of orifices having diameters of 0.020, 0.040, and 0.060 inch are shown in figure 5, where the flow rate per square foot of orifice area  $\rho_a V_a$  is plotted against  $\rho_a, 2^{h_B}$ , the product of the density and the pressure drop across the orifice. The density is based upon the static pressure on the discharge side of the orifice, so that

$$\rho_a, 2^{h_B} = \frac{(p_{a,1} - h_B) h_B}{RT_{a,n}}$$

Also shown in figure 5 are curves representing theoretical flows that would be obtained for flow nozzles with flow coefficients of 1.0 and 0.6. The portions of the theoretical curves that are linear are for subsonic flow through the orifice and were obtained from equation (5); the portions of the curves that are nonlinear are for supersonic pressure ratios across the orifice ( $h_B \geq 0.472p_a$ ) and were obtained from equation (5a). The linear portions of the curves are general for all temperatures and pressures, while the nonlinear portions are applicable only for the conditions of the orifice calibration.

It will be noted that the experimental results for all orifices that were tested lie along a curve parallel to the theoretical curves. This fact shows that the use of equations (5) and (5a) is satisfactory for calculating flow through these types of orifices for use at the root of transpiration-cooled turbine blades. The experimental flow coefficients  $B$  for the orifices investigated are given in the following table:

Orifice	Experimental flow coefficient, $B$
0.020-inch diam.	0.84
0.040-inch diam.	.84
0.060-inch diam.	.78
0.040-inch diam., upstream face chamfered	.87



Since the orifice diameter is used in the calculation of the flow coefficient  $B$ , the experimental values of flow coefficient are subject to error because of the difficulty in obtaining an accurate determination of the exact size of small orifices. The exact values of flow coefficient are relatively unimportant, anyway. The most significant conclusion that can be drawn from the results is that the small orifices drilled in plates, where the plate thickness was large relative to standard flat-plate orifice practice, behave in the manner predicted for flow nozzles. It is also of interest to note that chamfering the upstream face of an orifice increases the flow coefficient, as would be expected, but it does not affect the manner in which the flow varies with  $\rho_a, 2h_B$ .

#### Effect of Orifices in Series with Porous Surfaces on Permeability Correlation

By use of the procedure described in Calculation of Pressure Drops for Orifices in Series with Porous Walls, pressure drops were calculated for orifices and porous surfaces in series for ranges of flow rate, temperature, pressure, permeability, and orifice size in order to determine whether a method of correlation of the results would be possible. The results of these calculations are given in figure 6. It was found that

a plot of  $\frac{\mu_0^2 T_0}{\mu_{a,B}^2 T_{a,B}} (p_a^2 - p_g^2) \beta$  against  $\frac{\mu_0}{\mu_{a,B}} \rho_a v_a$ , which is the same plot used for correlating flow through porous surfaces without orifices in series (fig. 2), would correlate flow through orifices and porous materials in series within the accuracy of experimental data available for most cases.

In figure 6(a) is shown the effect of orifice size on flow for the case where the porous-material permeability was  $40 \times 10^{-9}$  inch. For this case the coolant-supply pressure  $p_a$  was 9600 pounds per square foot, and both the cooling-air temperature and the porous-surface temperature were  $740^\circ$  F. The curve in figure 6(a) for  $h_{B,\Omega}$  equal to zero (no orifice) is the same as the curve in figure 2. The value of the parameter  $h_{B,\Omega}$  indicates the orifice size. The larger the value of  $h_{B,\Omega}$ , the smaller the size of the orifice. As stated previously, the ratio  $h_{B,\Omega}/1440$  is approximately equal to the proportion of pressure drop through the orifice to the pressure drop from the coolant supply to the discharge on the outside of the porous surface. Figure 7 gives the relation between  $h_{B,\Omega}$ , the permeability  $12K'/\tau$ , and the ratio  $A_n B/A_a$  where  $A_a$  is the area of the porous surface being supplied by the

orifice having an area  $A_n$ . Figure 6(a) shows that, by the flow correlation method presented, decreasing the orifice size results in shifting of curves in the direction of lower flows, and the curves are essentially parallel to the curve for a porous material without an orifice in series.

Figure 6(b) shows the results of calculations to determine the effect of cooling-air and porous-wall temperatures on the method of correlation presented. The results are given for a value of  $h_{B,\Omega}$  of 1152 pounds per square foot, which would be a typical value to use for orifices in the base of turbine blades. This value corresponds to a pressure drop through the orifice of approximately four-fifths of the total pressure drop through the orifice and the porous wall.

For the case in which the cooling-air temperature is equal to the porous-wall temperature (no heat transfer), the temperature apparently does not affect the correlation, at least for the temperature range from 340° to 740° F. If, however, the blade wall is hotter than the cooling-air temperature, a shift in the curves results. Where calculations are to be made to determine the flow through orifices and porous material in series, it will be necessary, therefore, to account for the porous-wall and the cooling-air temperatures in the calculations.

Figure 6(c) shows the effect of pressure level on the correlation for two orifice sizes. The two coolant-supply pressures shown cover the expected range for turbine rotor blades for compressor pressure ratios from 4 to 10 and for flight altitudes from sea level to about 50,000 feet. Pressure level apparently has little or no effect on the correlation. The small break in the curve for  $h_{B,\Omega} = 1152$  pounds per square foot could result from inaccuracies in the data used for obtaining the correlation in figure 2. Thus it appears that the correlation of flow for various pressure levels is within the accuracy of experimental flow data.

Figure 6(d) shows the effect of various porous-material permeabilities on the correlation procedure for two values of  $h_{B,\Omega}$ . For the wide range of permeability  $12K'/\tau$  shown, the correlation is affected only slightly. Here again, as was the case with figure 6(c), inaccuracies in the original data (fig. 2) could easily result in the spread shown in figure 6(d).

The results of calculations shown in figure 6 indicate that the correlation procedure shown will provide a reasonable correlation for flow through orifices and a porous wall in series that will adequately

correlate all variables except wall temperature, when wall temperature is different from the cooling-air temperature. It appears, therefore, that if a cold-air experimental permeability correlation is available for a piece of apparatus having orifices and a porous surface in series, corrections must be made to the correlation curve if the results are to be used to predict coolant-flow rates for cases where the porous-wall temperature is different from the cooling-air temperature.

#### Effect of Permeability Variations on Coolant-Flow Rates and Porous-Wall Temperatures

Comparison of flow rates through porous surfaces with and without orifices in series. - The coolant-flow rates that might be expected for a wide range of pressure drop between the coolant-supply pressure and the coolant-discharge pressure are shown in figure 8 for temperature and pressure levels that might be expected in gas-turbine engines. Since it was shown in figure 6(d) that the permeability magnitude had little effect on the correlation for flow through a porous metal and orifices in series, the results shown in figure 8 should be fairly general. Note that the ordinate in figure 8 does not contain the term  $\beta$ ; therefore, the effect of pressure drop on flow rate can be read directly for constant porous-wall temperature. In figure 8(a) the dashed lines show how a 20-percent variation in permeability of the porous surface will affect the coolant-flow rate for a porous wall in series with an orifice of such diameter that  $h_{p,\Omega} = 1152$  pounds per square foot for an average permeability of  $40 \times 10^{-9}$  inch. Over the range of pressure drop shown, a 20-percent variation in permeability can result in coolant-flow variations from about 20 to 40 percent for constant porous-wall temperature.

For the case where there are no orifices in series with a porous surface, the same coolant-flow rates can be obtained for given coolant-supply and discharge pressures as were obtained with orifices, if the permeability is decreased by the proper amount. The solid lines in figure 8(a) show how the coolant flow varies with pressure drop for a 20-percent variation in permeability for flow without orifices. The basic permeability for this case will result in the same coolant-flow rate as was obtained with permeability of  $40 \times 10^{-9}$  inch with an orifice in series for a pressure drop corresponding to  $0.34 \times 10^6$   $\text{lb}^2/\text{ft}^4$  on the ordinate scale. Over the range of pressure drop shown, a 20-percent variation in permeability will result in coolant-flow variations of approximately the same magnitude as for the case where the flow was through an orifice and a porous material in series.

2979

In figure 8(b) is shown the coolant-flow variation for random permeability variations of  $\pm 20$  percent for surfaces with two different average permeabilities being fed by an orifice of the same size as used in figure 8(a). The values of average permeability shown are extreme, because they are the same as the limiting values of the local permeability variations that were considered. Significant in figure 8(b) is the fact that, as the average permeability varies from  $32 \times 10^{-9}$  to  $48 \times 10^{-9}$  inch, the coolant-flow rate for the basic permeability of  $40 \times 10^{-9}$  inch varies from approximately 45 to 65 percent. It is important, therefore, that the average permeability of a surface being fed by an orifice be known, in order to be able to calculate the local coolant flows resulting from local permeability variations. A 20-percent variation in permeability changes the coolant-flow rate approximately the same amount from that for the basic permeability, regardless of average permeability.

Comparison of temperature and flow variations for porous surfaces with and without orifices in series. - The effects of the flow variations shown in figure 8 on blade temperature are given in figure 9(a) for a turbine-inlet gas temperature of  $2500^{\circ}$  F and a gas Reynolds number of  $2 \times 10^5$ . The ratio of local coolant flow to design coolant flow is also shown. The design coolant flow is specified as the amount that would be required to obtain a blade temperature of  $1000^{\circ}$  F.

It can be observed that, for a porous wall in series with an orifice of diameter such that  $h_{B,\Omega} = 1152$  pounds per square foot for an average permeability of  $40 \times 10^{-9}$  inch, a 20-percent variation in permeability can result in a maximum variation in local blade temperature of about  $325^{\circ}$  F, if the average permeability is equal to the design or specified permeability. If no orifice is used and if the porous-material permeability is reduced to obtain the same coolant flow as obtained with an orifice and a material having a permeability of  $40 \times 10^{-9}$  inch, a 20-percent variation in permeability will result in approximately the same variations in coolant flow and blade temperature. If, however, the average permeability is different from the specified permeability, the coolant-flow and blade-temperature variations may be greatly increased when orifices are used in series with the porous surface. If the local permeability were found to be 20 percent lower than the specified permeability and the average permeability were at the same time higher than the specified permeability, the blade could experience local overheating by as much as  $600^{\circ}$  F. These results neglect the effect of wall conduction, which could in some cases reduce temperature variations due to random variations in permeability. For thin walls, however, the effect of conduction would probably be small.

As will be shown later, the results in figure 9(a) can be generalized to a considerable degree to include other permeabilities; therefore it can be concluded that the incorporation of orifices in series with a porous wall does not improve blade-temperature and coolant-flow variations that can result from random variations in permeability in a surface being fed from a single orifice. In fact, in many cases the temperature and coolant-flow variations can become much worse. Therefore, it is indicated that, for turbine blades constructed in a manner similar to that shown in figures 1 and 3, as much care, or more, is required to obtain the proper permeability distribution in a spanwise direction with blades incorporating orifices at the base as for blades that do not utilize orifices. The use of orifices is still of considerable advantage in controlling coolant flows in a chordwise direction and in accounting for effects of flight altitude as discussed in reference 2. In addition, unwanted permeability variations in a chordwise direction can, in many cases, be corrected by use of orifices of the proper size.

Effect of random permeability variations on blade temperature and coolant flow for various conditions. - It was shown in figure 9(a) that a knowledge of the average permeability of a porous surface being fed from an orifice must be known in order to calculate the effects of permeability variations on coolant flows and blade temperatures. It was also shown that, if the average permeability is the same as the specified permeability, a given percentage variation in permeability will have approximately the same effect on coolant flow and blade temperature, regardless of whether orifices are placed in series with the porous wall or not. The results shown in figures 9(b) to (d) will, therefore, be shown for no orifices in series with the porous wall. These results are independent of coolant pressure level, and, although the results are for no orifices, they will indicate about the best that can be obtained with orifices in series with the porous wall.

Figure 9(b) shows the effect of permeability variations on blade temperature and coolant-flow rates for various magnitudes of specified permeability, for turbine-inlet temperatures of 1600° and 2500° F, and for a gas Reynolds number of  $2 \times 10^5$ . Values of specified permeability from  $20 \times 10^{-9}$  to  $60 \times 10^{-9}$  inch were chosen. This is a very wide range of permeability and should adequately cover any requirements for gas-turbine blades. A random variation from specified permeability has approximately the same effect on coolant flows and blade temperatures for the complete range of specified permeabilities considered, although it is shown that there is a slight advantage in being able to utilize a lower specified permeability. The turbine designer, however, does not have a completely free choice of permeabilities to use in turbine blades. The coolant-discharge pressure  $p_g$  is set by the engine cycle, and there are penalties such as an auxiliary compressor and high cooling-air temperature

associated with high coolant-supply pressures. It is necessary, therefore, to tailor the permeability and orifice size to the quantity of flow required and the available coolant-supply pressure. If the designer chooses a relatively low porous-wall permeability in order to capitalize on the slight gains in temperature variation shown in figure 9(b), it may mean that the required metering orifice will be so large that some of the advantages of using orifices to improve off-design cooling performance will be cancelled. The gains shown in figure 9(b) due to using a lower permeability are probably so slight that no special consideration should be given to lower permeabilities in cooled-turbine design.

Figure 9(b) also shows the effect of turbine-inlet gas temperature. Transpiration cooling will probably be utilized mostly at high turbine-inlet temperatures. For a given gas Reynolds number, random variations in permeability will have a much greater effect on blade temperature for high gas temperatures than for low gas temperatures, even though the effect on the ratio of local-to-design coolant flow is smaller for high gas temperatures. Permeability variations of over 5 to 10 percent are probably excessive at a turbine-inlet temperature of 2500° F. It is also of interest to note that, for a turbine-inlet temperature of 2500° F, more than  $3\frac{1}{2}$  times as much coolant flow is required to cool the blades to a temperature of 1000° F than is required for a turbine-inlet temperature of 1600° F.

Figure 9(c) shows how permeability variations affect blade temperature for a turbine-inlet temperature of 2500° F, design blade temperatures of 1000° and 1500° F, and a specified permeability of  $40 \times 10^{-9}$  inch. There is not a very great difference in temperature variation for the two design temperatures, except in the range where the permeability variations are of such magnitude that the temperature variations probably could not be tolerated anyway. It is of interest to note that the blade temperature does not behave exactly in the manner that would be indicated by the coolant-flow rates. Observation of the coolant flows indicates that for a 20-percent minus variation in permeability, the blade designed for 1000° F should probably have less temperature variation than the blade designed for 1500° F blade temperature. The opposite is true, and although the reason is not obvious, it probably occurs because of the difference between the gas and blade temperature levels and because of the difference in magnitude of the coolant-flow rates. The coolant-flow requirement for the blade cooled to 1000° F is more than twice that required to cool the blade to a temperature of 1500° F. This same trend was shown in reference 2, and it indicates the savings in cooling-air flow that are possible if porous materials are developed that will permit higher blade temperatures.

Figure 9(d) shows the effect of gas Reynolds number on blade temperature and coolant flow as the permeability varies for a turbine-inlet temperature of 1600° F, a specified blade temperature of 1000° F, and a

specified permeability of  $40 \times 10^{-9}$  inch. The lower the Reynolds number, the greater will be the blade temperature variations for given variations in permeability. These results have a double significance. The Reynolds number increases as the distance  $x$  along the blade chord increases and as the flight altitude decreases. It is indicated, therefore, that, for turbulent-boundary-layer flow, slightly greater care is required in controlling spanwise permeability variations near the blade leading edge than near the blade trailing edge, and blade temperature variations will be somewhat higher at high altitudes than at low altitudes. In addition, note the coolant flows required to obtain a design blade temperature of  $1000^{\circ}$  F for various Reynolds numbers; increasing the Reynolds number by a factor of 100 results in an increase of coolant flow by a factor of only 42. Since, for a change in flight altitude, the gas Reynolds number is directly proportional to the combustion-gas flow through the engine, these results show that the ratio of cooling-air flow to combustion-gas flow (coolant-flow ratio) increases as flight altitude is increased. This trend was also shown in reference 2. The results given herein indicate trends only and do not give values of the coolant-flow ratio required for gas-turbine engines. Coolant-flow requirements for an engine having a compressor pressure ratio of 4 for turbine-inlet gas temperatures of  $1600^{\circ}$  and  $2500^{\circ}$  F are given in reference 2.

The results of figures 9(b) to (d) can be summarized by stating that care will be required in the fabrication of transpiration-cooled turbine blades to minimize permeability variations in a spanwise direction. Greater care is required for high than for low turbine-inlet temperatures. In order to keep temperature variations less than  $\pm 100^{\circ}$  F, a permeability variation of not over  $\pm 6$  percent is required for a gas-turbine-inlet temperature of  $2500^{\circ}$  F and not over  $\pm 10$  percent for a turbine-inlet temperature of  $1600^{\circ}$  F. Operation at high gas Reynolds numbers or low specified permeabilities will permit somewhat greater local permeability variations.

#### Evaluation of Experimental Porous Blade

The experimental porous blade shown in figure 1 was flow-tested statically in the fixture shown in figure 1(c) to determine permeability variations resulting in the blade from the fabrication procedure used. The results of these static flow checks were then used to calculate the blade-temperature and coolant-flow distributions expected for this blade under the design operating conditions. The results of these experiments and calculations are shown in figures 10 to 12.



Effect of orifices and coolant-passage pressure losses on blade permeability measurements. - The calculated effect of orifices of various sizes on the permeability correlation for flow through orifices and a porous surface in series is shown in figure 6. In order to determine whether this calculated trend would actually occur in a transpiration-cooled blade as shown in figure 1, experimental permeability data were obtained for several positions on the blade with and without the orifice plate at the blade base. The data for one of these positions, which are representative of all data taken, are shown in figure 10. The data indicated by the circles were obtained with no orifice plate and would correspond to  $h_{B,\Omega}$  equal to zero in figure 6(a). For reference, the zero line from figure 6(a) is also shown in figure 10. The experimental permeability correlation line for this blade does not exactly coincide with the basic permeability curve used for the calculations in this report. This difference is presumably due to a slight difference in the flow characteristics for sintered materials and wire cloth. The basic line was obtained from reference 3 for wire cloth. A comparison made with the experimental data from the sintered material in reference 4 indicated a similar change in slope of the correlation curve. This small change in slope of the correlation lines for two types of porous material should not affect the trend of the results shown in figures 6 to 9.

The data indicated by the triangles in figure 10 were obtained with the orifice plate in place at the blade base. The size of the orifices corresponded to a value of  $h_{B,\Omega}$  equal to 1200 pounds per square foot. With the experimental permeability curve indicated by circle data points and with  $h_{B,\Omega} = 1200$  pounds per square foot, calculations were made to predict the flow correlation with orifices. The close agreement between the analytically predicted line and the data line indicated by the triangles gives a partial verification to the calculation procedure used in this report.

In order to determine the effects of pressure losses through the coolant passage on the coolant flow through a porous surface, experiments were made with both a short and a long coolant-flow path, and the results were compared. The data shown in figure 10 are for a position near the blade tip, so that the coolant-flow passage is normally about  $4\frac{1}{2}$  inches long. Data were also taken at exactly the same location on the blade with the coolant entering the blade at the tip instead of the root, so that the coolant-flow passage was only  $1\frac{1}{2}$  inch long. The data for this case are indicated by the squares in figure 10. It can be seen that slightly less cooling air flows through the position on the blade investigated when the coolant passage is short than when the coolant passage is long. Although as the passage length is changed the change

in coolant flow is so slight that there would be negligible effect on blade temperature, an indication of the mechanism of the flow distribution along a porous wall is shown. From studies of flow through holes located along the length of pipes, it has been shown that for high fluid velocities the flow through the holes farthest from the entrance is highest, because the momentum of the fluid tends to keep it flowing along the pipe. The trend is the same for a porous wall fed by a coolant passage similar to those in the porous blade investigated. A rough calculation indicated that, with total-pressure losses neglected, the static-pressure distribution that would result due to the bleeding off of cooling air along the passage through the porous wall would result in a much greater change in coolant flow than was shown in figure 10. It can be concluded, therefore, that there is a compensating effect between the static-pressure distribution and the pressure losses through the coolant passage. For this particular blade, these two effects were almost equal. Tests made at other locations on the blade also showed a similar trend.

The results shown are for static conditions. For turbine rotor blades, centrifugal force would tend to cause more of the air to be forced out near the tip of the blade than was measured in the static tests. Calculations have not been made to determine the magnitude of this effect; but, if it is serious, three possible solutions are (1) to vary the permeability in a spanwise direction to compensate for the higher static pressures near the blade tip, (2) to decrease coolant-passage area to cause higher pressure losses along the passage length, or (3) to increase pressure losses by means of a restriction such as loosely packed metal wool in the coolant passage. Further studies are required in order to determine the relative merits of the three systems. Off-design operation at both high altitudes and low engine speeds must be considered in order to determine whether the temperature distribution along the passage length would be acceptable at all engine conditions.

Permeability variations over blade surfaces. - The local permeabilities were measured around the periphery of the experimental blade at three spanwise locations both with and without the orifices at the blade base. The results of these measurements are shown in figure 11. The measurements made without the orifices in the base are indicated by  $12K'/\tau$ , and the measurements made with the orifices in the base are indicated by  $(12K'/\tau)_{ap}$ . For reference, the corresponding values of  $h_{B,\Omega}$  that resulted because of the orifice sizes used are also shown in the figure.

Figure 11(a) shows very large variations in permeability along the blade chord. Since orifices of various sizes can be installed at the various locations along the blade chord, the chordwise permeability

variation without orifices probably would not be too serious if the permeabilities were high enough at all locations to obtain an adequate amount of flow. It will be shown, however, that the permeabilities at the leading and trailing edges of the blade tested are much too low.

In a spanwise direction, the permeability variations should be somewhat lower than were obtained. As indicated in figure 9, the maximum variation should probably be from 5 to 10 percent. In some cases, the spanwise permeability variations in the experimental blade are on the order of  $\pm 20$  percent (a maximum variation of about 40 percent). Therefore, it would appear that, particularly for high-temperature application, a somewhat better spanwise permeability control may be required than was obtained on this particular experimental blade.

Shown in figure 11(b) are the apparent permeability values obtained with orifices at the blade base. It was specified that the apparent permeability on the suction surface should be  $8.7 \times 10^{-9}$  inch, and on the pressure surface  $10.4 \times 10^{-9}$  inch. The resulting blade was much less permeable than was specified. On the suction and pressure surfaces, the proper apparent permeabilities could probably have been obtained with a better choice of orifice sizes over most of the surfaces. Difficulty would have been encountered at the trailing edge, however, because the permeabilities without orifices are not even as high as the specified apparent permeabilities.

At the blade leading edge, the apparent permeability was specified to be  $14.2 \times 10^{-9}$  inch. Experimental measurements were not made directly at the leading edge, but, from the trend of the curves of  $12K'/\tau$ , the blade leading edges are much too dense.

Effect of permeability variations on coolant flow and blade temperature. - The original specifications for the experimental blade were for permeabilities that would be approximately suitable for operation at a gas temperature of  $1600^{\circ}$  F and a coolant temperature of  $340^{\circ}$  F. Figure 9(b) shows that much larger variations in permeability can be tolerated at this gas temperature than could be tolerated at a higher gas temperature (on the order of  $2500^{\circ}$  F). In order to determine analytically how the experimentally measured apparent permeability variations would affect blade temperatures and coolant flows, it was assumed that the coolant-supply pressure was set so as to obtain a specified blade temperature of  $1000^{\circ}$  F for the specified permeability. It was also assumed that the pressures were different on the suction and pressure surfaces, but that there was no pressure gradient along the blade chord. This assumption would approximately correspond to an impulse blade. The gas Reynolds number was assumed to be  $5 \times 10^5$ .

The coolant flow required to obtain a specified blade temperature is dependent only upon the gas Reynolds number, the gas temperature, and the coolant temperature; it is not dependent upon the blade permeability. The permeability determines the coolant-supply pressure that is required to obtain a given coolant flow. If, however, the coolant-supply pressure is a set value, then the coolant flow is dependent upon the permeability, and this flow in turn affects the blade temperature.

With the preceding temperature and Reynolds number assumptions, calculations were made for two cases: (1) the coolant-supply pressure and the pressure on the outside surface of the blade are such that a coolant flow will be obtained that will result in a 1000° F blade temperature for the originally specified values of apparent permeability of  $8.7 \times 10^{-9}$  inch on the suction surface and  $10.4 \times 10^{-9}$  inch on the pressure surface; and (2) higher pressure differences between the coolant and the gas are specified, so that a 1000° F blade temperature will be obtained for the averages of the experimentally measured apparent permeabilities, which are  $4.5 \times 10^{-9}$  inch on the suction surface and  $7.5 \times 10^{-9}$  inch on the pressure surface. The blade temperature distributions and the ratio of actual-to-design coolant-flow distributions that were calculated for these two cases are shown in figure 12.

Figure 12(a) shows the results of calculations for case (1). Since the experimentally measured apparent permeabilities were all less than those specified, the coolant-flow rates are all too low; that is, they are less than the design values. Therefore the blade temperatures are all above 1000° F. The range of blade temperature is from 1020° F to 1210° F, or an integrated average blade temperature of 1100° F. Direct measurements were not made at the leading and trailing edges, but it would be expected that considerably higher temperatures would occur in those regions. The temperature variations that would occur in this blade are probably tolerable, but the temperature level is too high for materials such as stainless steel. At these temperatures, oxidation would soon block off the coolant flow through the porous wall.

The coolant-flow distribution is also shown in figure 12(a). The coolant flow behaves in a manner inverse to the blade temperature. The average coolant flow for these conditions was only 61 percent of the design value that would have been obtained if the blade had had the proper permeability.

Figure 12(b) shows the results of calculations for case (2). In this case it was assumed that the permeabilities had been specified as the average of the experimental values, which would then result in an

2979

average blade temperature of  $1000^{\circ}$  F and average ratio of local-to-design coolant flow of 1.0. The specification of lower permeabilities for case (2), in order to correspond to the average values obtained in the fabrication ( $4.5 \times 10^{-9}$  in. on suction surface and  $7.5 \times 10^{-9}$  in. on pressure surface), would result in the requirement of higher coolant pressures; however, compressor discharge pressure would probably be sufficient. For this case it will be observed that the variations in temperature along the blade are higher than they were for the higher specified permeabilities; and, although part of the blade is now cooled to temperatures below  $1000^{\circ}$  F, the hottest portion of the blade has been cooled only  $50^{\circ}$  F; therefore, portions of the blade could still overheat to a dangerous degree.

When it is assumed that these hot spots could be eliminated by a better choice of orifice sizes, it is observed that there would still be spanwise temperature variations of considerable magnitude. If this blade were to operate at a higher gas temperature level, the temperature gradients would be much more severe than shown in figure 12, and much smaller variations in permeability could be tolerated.

If the coolant-supply pressure were raised high enough, all portions of the experimental blade could possibly be cooled to a temperature of  $1000^{\circ}$  F or less. This pressure would be impractical, however, because a cooling-air compressor pressure ratio of approximately 12 would be required (for an engine compressor pressure ratio of 4) if the cooling-air temperature were held to  $340^{\circ}$  F by some refrigeration system. If the cooling-air temperature were the same as the compressor discharge temperature, it would be impossible to cool the blade to a maximum temperature of  $1000^{\circ}$  F, because the compressor pressure ratio would be so high that the cooling-air temperature would exceed  $1000^{\circ}$  F.

#### Design Features for Transpiration-Cooled Turbine Blades

From the results of this study, from reference 2, and from experience gained in the fabrication of air-cooled gas-turbine blades, the following features can be suggested as either desirable or necessary in the fabrication of transpiration-cooled blades that will be suitable in gas-turbine engines:

(1) Blades utilizing orifices in the blade base are highly desirable, because the orifices improve the off-design cooling performance of the blades and permit a much greater degree of freedom in the manufacturing techniques. The blades can have a blade shell of uniform permeability (in a chordwise direction at least), or unwanted chordwise variations in permeability can be corrected by the orifices as indicated to some degree in figure 11.

(2) In most cases the permeability of the porous shell should be so chosen that when an orifice of the proper size is used to obtain the required apparent permeability, the value of  $h_{B,\Omega}$  will be within the approximate range from 1000 to 1400 pounds per square foot. A relation between shell permeability, apparent permeability, and  $h_{B,\Omega}$  is given in figure 13. From these values and figure 7, the approximate orifice size can be determined. The final orifice size will probably have to be determined experimentally.

(3) Accurate velocity distributions over the surface of the turbine blades will be required in order to determine the proper apparent permeability requirements for turbine blades. The design of each blade will have to be tailored to the engine in which it is to be used.

(4) In calculating the required coolant-flow distribution over the surface of the blades, it is recommended that reference 12 be used for regions close to the blade leading edge and that reference 2 be used for all other locations on the blade. It should be noted, however, that equation (1) in reference 2 should be replaced by equation (11) in the present report. These recommendations on methods of calculating coolant-flow requirement are based on judgement rather than experience, because as yet no experimental verification has been obtained in a gas-turbine engine.

(5) For both turbine rotor and stator blades, the porous wall should be quite thin (on the order of 0.020 in. if possible), so that the leading and trailing edges of the blade can be adequately cooled.

(6) The strut inside the blade should have the coolant passages arranged to obtain equitable coolant-flow distribution to the entire blade. Sketches of the coolant-passage arrangement for the experimental blade tested and for a more desirable passage arrangement are shown in figure 14. The spacing of the fins on the strut is probably more a function of the support required for the shell than it is a function of cooling considerations. With respect to cooling, at least half the fins shown in figure 14(a) can be eliminated to obtain a configuration more like figure 14(b). Also note the different arrangement of the passages at the blade leading and trailing edges to provide better coolant-supply paths.

(7) For turbine stator blades, the primary purpose of the strut will be to divide the blade into compartments for the purpose of metering the cooling air through orifices. For turbine rotor blades, the strut will also serve as the support structure for the porous shell. In order to reduce the strut stresses as much as possible, a large amount of taper will be required in the strut in a spanwise direction. It will also be desirable to taper the aerodynamic contour of the rotor blade in order to shorten the supporting fins towards the tip of the strut for two

purposes: (1) to further reduce stresses in the strut, and (2) to increase the pressure losses in the outer portion of the coolant passage in order to obtain a more uniform distribution of cooling air along the blade span.

#### SUMMARY OF RESULTS

The results of this analytical and experimental investigation of random permeability variations can be summarized as follows:

1. A calibration of small orifices where the orifice plate thickness was large compared to standard flat-plate orifice practice showed that the orifice behaved in the manner predicted for flow nozzles.

2. Analytical investigation of the coolant flow through orifices and a porous material in series showed that the manner that has been used for correlating flow through porous materials without orifices in series will probably account for all variables except wall temperature when the wall temperature is different from the cooling-air temperature. The analytical investigation was partially verified by experiment.

3. Random permeability variations in a porous surface being supplied coolant from a common source can result in substantial variations in local coolant-flow rates and local wall temperatures. In order to keep temperature variations to less than  $\pm 100^{\circ}$  F for a specified blade temperature of  $1000^{\circ}$  F, while neglecting effects of wall conduction, a permeability variation of not over  $\pm 6$  percent is required for a turbine-inlet gas temperature of  $2500^{\circ}$  F, and not over  $\pm 10$  percent for a turbine-inlet temperature of  $1600^{\circ}$  F. Operation at high gas Reynolds numbers or low permeabilities will permit somewhat greater local permeability variations. The use of orifices in series with the porous surface does not reduce temperature variations due to variations in permeability. In fact, in some cases the temperature variations are higher than for the case where the porous wall does not have an orifice in series.

4. Evaluation of an experimental transpiration-cooled blade indicates that unless substantial pressure losses occur in the coolant passage or unless lower permeabilities are used near the blade tip, a greater amount of cooling air will probably flow out near the tip of the blade than near the blade root.

5. The fabrication method used on the experimental transpiration-cooled turbine blade provided a means whereby a thin, porous, sintered shell can be attached to a central strut; however, the attachment method



must be investigated under conditions of high rotational speed, and the random permeability variations in the blade were greater than could be tolerated in a turbojet engine.

6. The use of a strut inside transpiration-cooled turbine blades is highly desirable in order to support the blade adequately and to divide the blade into compartments to permit the use of orifices to meter the cooling air to the various locations around the blade periphery. Care is required in the design, however, in order to ensure acceptable strut stress levels, proper coolant-passage areas, and proper coolant-flow distribution.

Lewis Flight Propulsion Laboratory  
National Advisory Committee for Aeronautics  
Cleveland, Ohio, July 20, 1953

2979

## APPENDIX - SYMBOLS

The following symbols are used in this report:

A	flow area, sq ft
B	flow coefficient for flow nozzle
C	constant
g	acceleration due to gravity, ft/sec <sup>2</sup>
h <sub>B</sub>	pressure drop through orifice, lb/sq ft
K'	permeability coefficient, sq ft; for $(p_a - h_B)^2 - p_g^2 = 3556^2 - 2116^2$ , lb <sup>2</sup> /ft <sup>4</sup>
P	barometric pressure, lb/sq ft
Pr	Prandtl number
p	static pressure, lb/sq ft abs
R	gas constant, ft-lb/(lb)(°F)
Re <sub>g</sub>	Reynolds number with fluid properties based on gas temperature, $\rho_g V_g x / \mu_g$
r	ratio of velocities in boundary layer (eq. (7))
T	temperature, °R
V	velocity, ft/sec
v	flow volume per unit surface area and time, ft/sec
x	distance from blade leading edge, ft
β	factor used for correlating permeability data; $\beta = C/\tau$ , ft <sup>-1</sup>
γ	ratio of specific heats
μ	absolute viscosity, lb-sec/sq ft
ρ	density, lb/cu ft
τ	thickness, ft

$$\phi = \frac{71.3(\rho_a v_a) \text{Pr}_g^{2/3}}{r \text{Re}_g^{0.9}} \left( \frac{x}{g \mu_g} \right) \quad (\text{see eq. (10)})$$

## Subscripts:

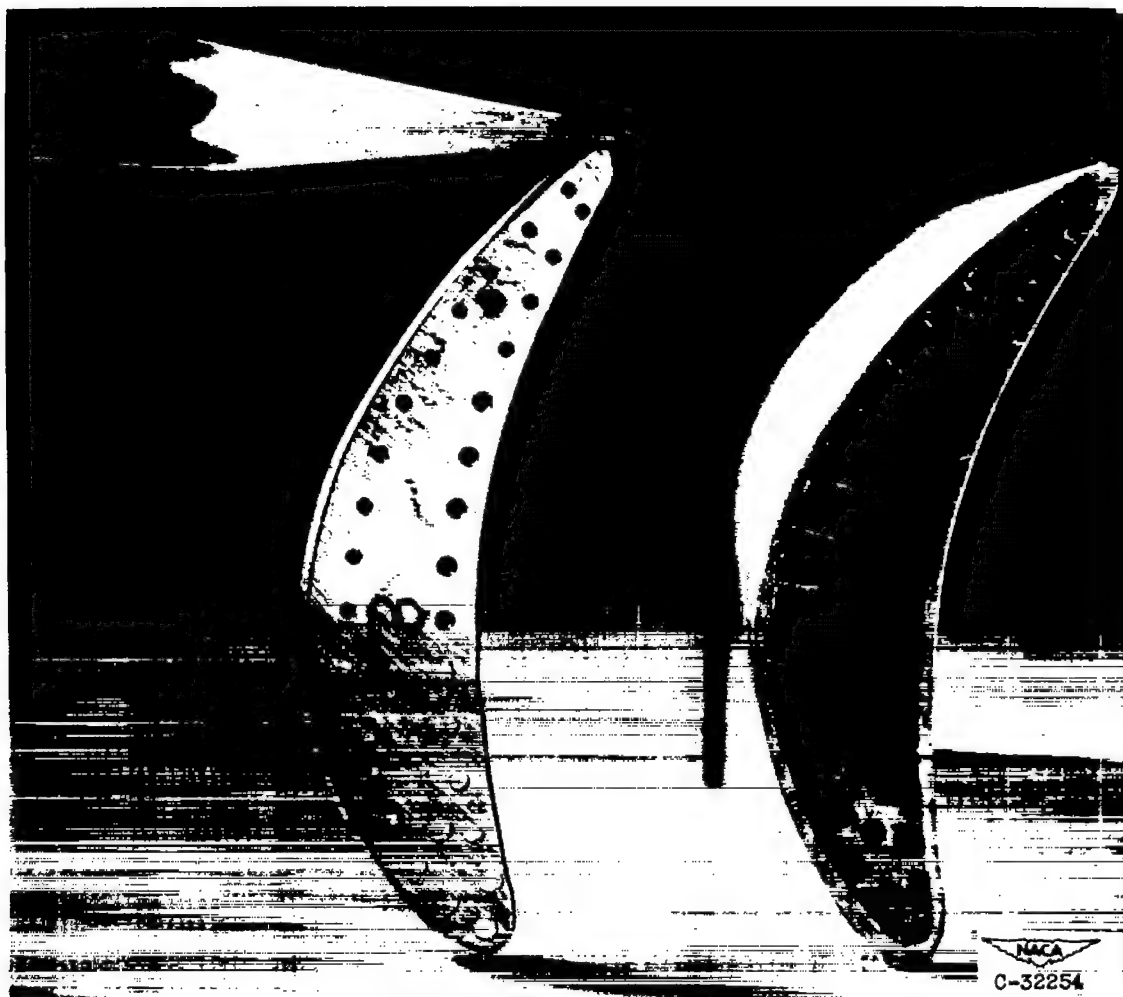
- a cooling air or surface through which cooling air is passing
- ap refers to apparent permeability measurement that includes effect of orifices in series with porous wall
- av refers to average permeability over an area being supplied by an orifice of some specified size
- B blade (local conditions) or refers to blade wall temperature
- d indicates a design condition
- e effective
- g combustion gas
- i turbine inlet
- n orifice (or flow nozzle)
- std designates specified permeability, and orifice size corresponding to specified permeability
- $\Omega$  designates a standard set of flow conditions for specifying permeability and orifice constant
- 0 for reference temperature of 518.4° R
- 1 upstream of orifice
- 2 downstream of orifice

## REFERENCES

1. Eckert, E. R. G., and Livingood, John N. B.: Comparison of Effectiveness of Convection-, Transpiration-, and Film-Cooling Methods with Air as Coolant. NACA TN 3010, 1953.
2. Esgar, Jack B.: An Analytical Method for Evaluating Factors Affecting Application of Transpiration Cooling to Gas Turbine Blades. NACA RM E52G01, 1952.
3. Donoughe, Patrick L., and McKinnon, Roy A.: Experimental Investigation of Air-Flow Uniformity and Pressure Level on Wire Cloth for Transpiration-Cooling Applications. NACA RM E52E16, 1952.
4. Bartoo, Edward R., Schafer, Louis J., Jr., and Richards, Hadley T.: Experimental Investigation of Coolant-Flow Characteristics of a Sintered Porous Turbine Blade. NACA RM E51K02, 1952.
5. Probst, R. L.: Investigation of Sintered Loose Spherical Powder for Fabrication into Transpiration Cooled Turbine Blades. Prog. Rep. No. 9, Federal-Mogul Res. and Dev. Div., Federal-Mogul Corp., Dec. 28, 1952. (Bur. Aero., U. S. Navy Dept. Contract No. NOas 51613-C.)
6. Anon.: Fluid Meters, Their Theory and Application. A.S.M.E. Res. Pub., Fourth ed., pub. by Am. Soc. Mech. Eng. (New York), 1937.
7. Friedman, Joseph: A Theoretical and Experimental Investigation of Rocket-Motor Sweat Cooling. Jour. Am. Rocket Soc., no. 79, Dec. 1949, pp. 147-154.
8. Eckert, E. R. G., and Esgar, Jack B.: Survey of Advantages and Problems Associated with Transpiration Cooling and Film Cooling of Gas-Turbine Blades. NACA RM E50K15, 1951.
9. Koffel, William K.: Preliminary Experimental Investigation of Transpiration Cooling for an Afterburner with a Sintered, Porous Stainless-Steel Combustion-Chamber Wall. NACA RM E53D08, 1953.
10. Lees, Lester: Stability of the Laminar Boundary Layer with Injection of Cool Gas at the Wall. Rep. No. 124, Aero. Eng. Lab., Princeton Univ., May 20, 1948. (Tech. Rep. No. 11, Proj. Squid, under Navy Dept. Contract N6-ORI-105, T. O. III, Phase I, NR 220-038.)
11. Keenan, Joseph H., and Kaye, Joseph: Gas Tables. John Wiley & Sons, Inc., 1948.
12. Eckert, E. R. G., and Livingood, John N. B.: Method for Calculation of Heat Transfer in Laminar Region of Air Flow Around Cylinders of Arbitrary Cross Section (Including Large Temperature Differences and Transpiration Cooling). NACA Rep. 1118, 1953. (Supersedes NACA TN 2733.)

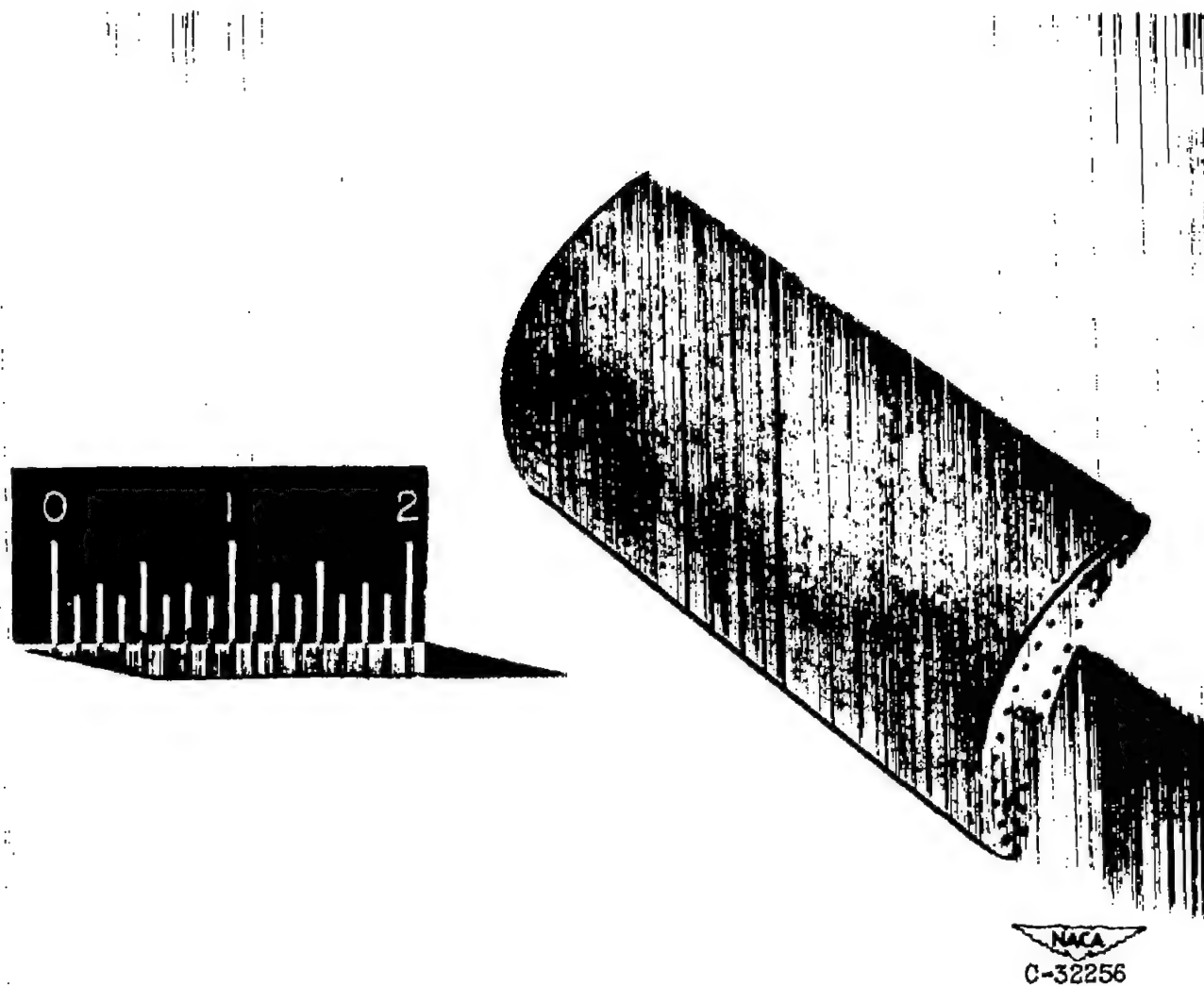
2979

CP-5 back



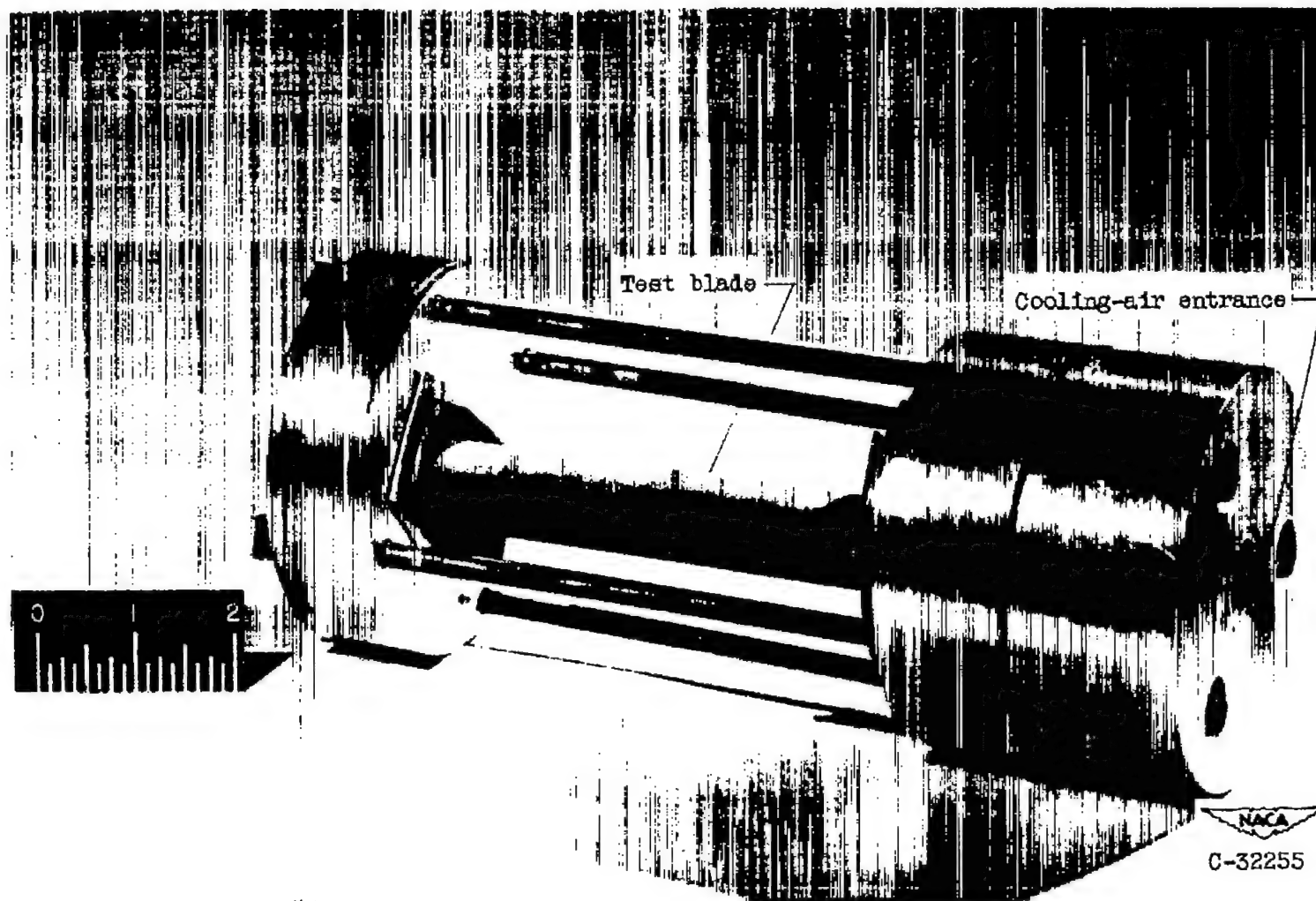
(a) Close-up view showing strut support inside blade and orifice plate for metering cooling air to each passage.

Figure 1. - Sintered, porous turbine blade fabricated for static permeability investigations.



(b) View showing orifice plate attached to blade root.

Figure 1. - Continued. Sintered, porous turbine blade fabricated for static permeability investigations.



(c) Blade installed in holder of permeability test rig.

Figure 1. - Concluded. Sintered, porous turbine blade fabricated for static permeability investigations.



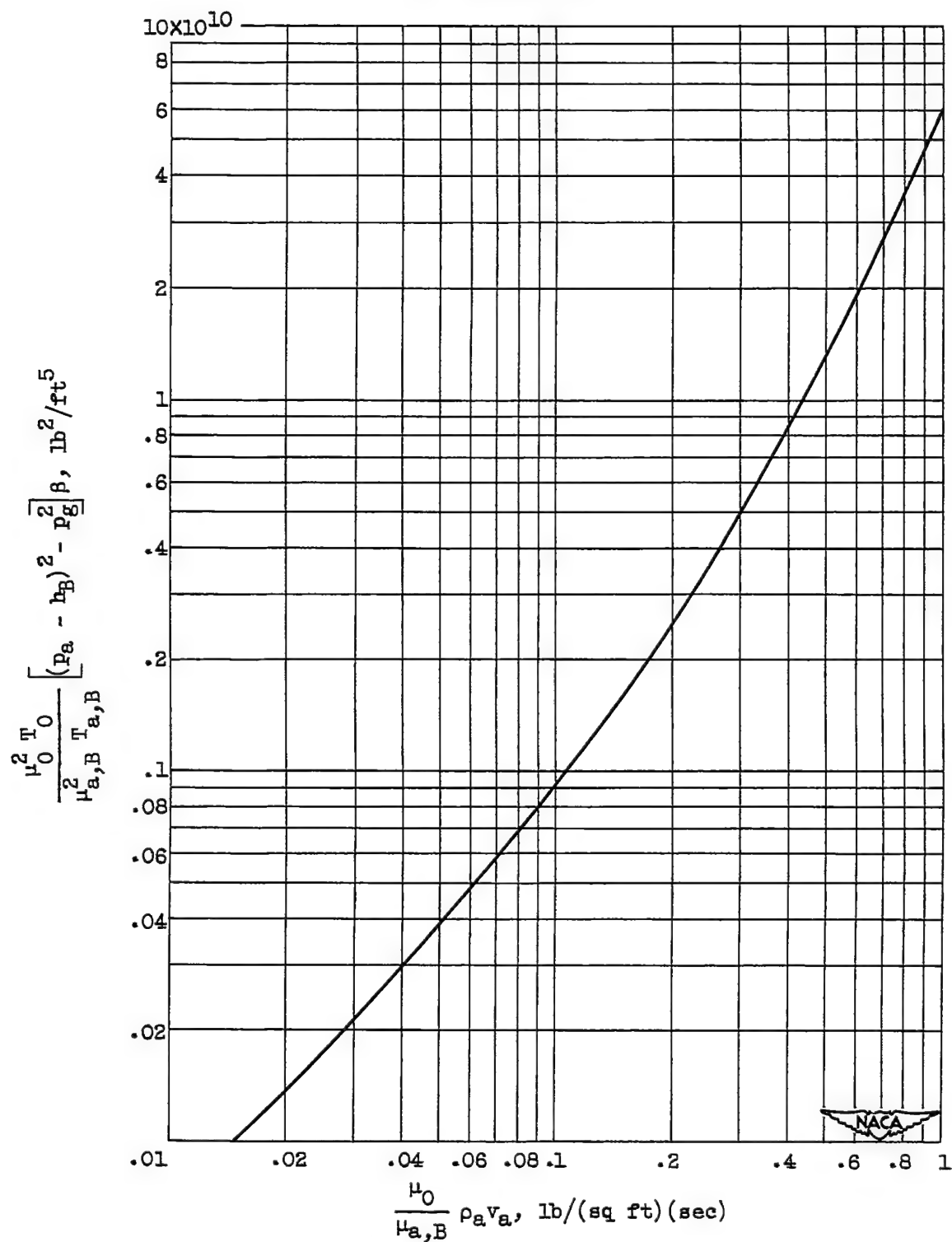


Figure 2. - Permeability correlation for all porous materials used in analysis.

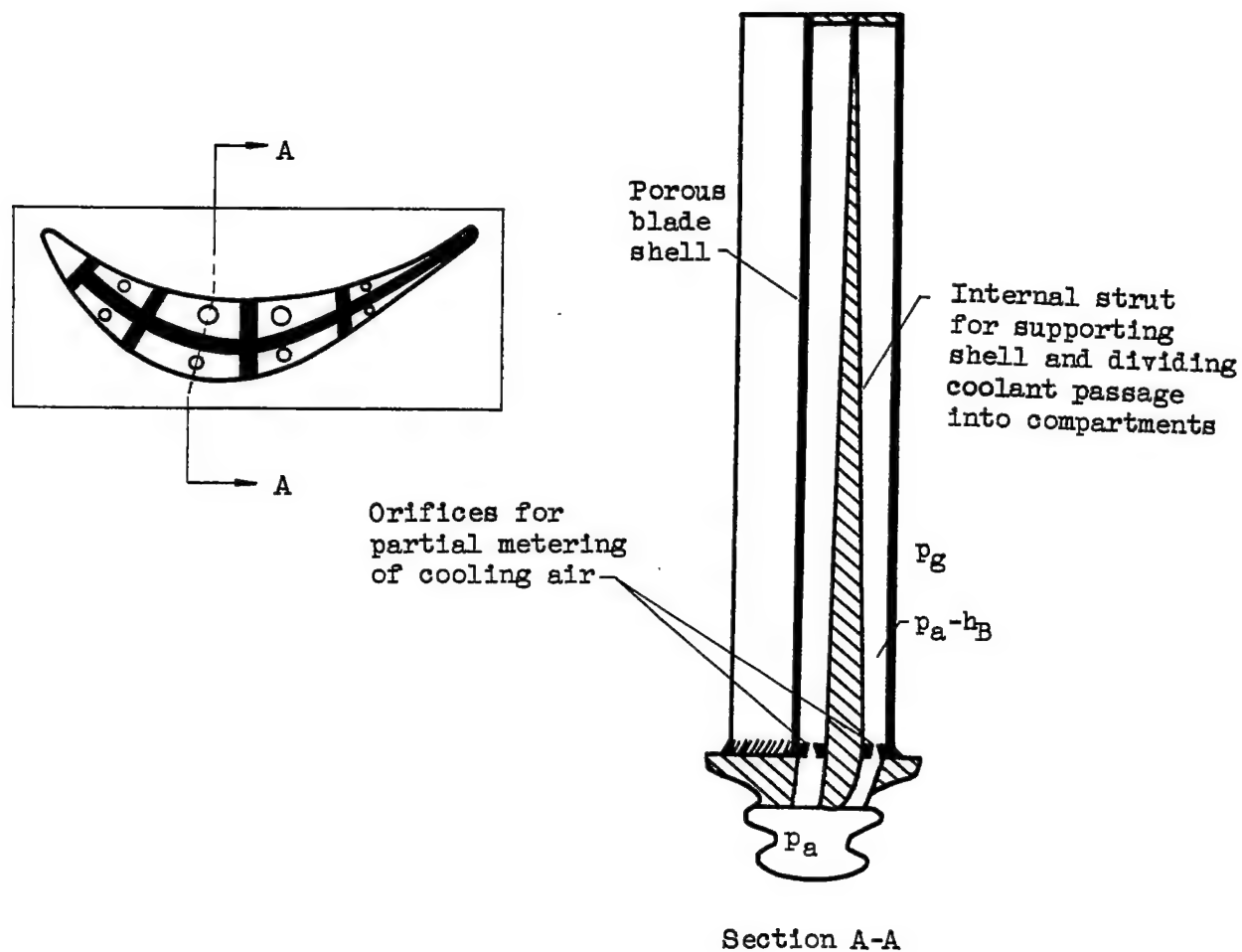
~~CONFIDENTIAL~~

Figure 3. - Sketch of strut-supported, transpiration-cooled turbine blade utilizing multiple orifices at blade base for partial metering of cooling air.

~~CONFIDENTIAL~~

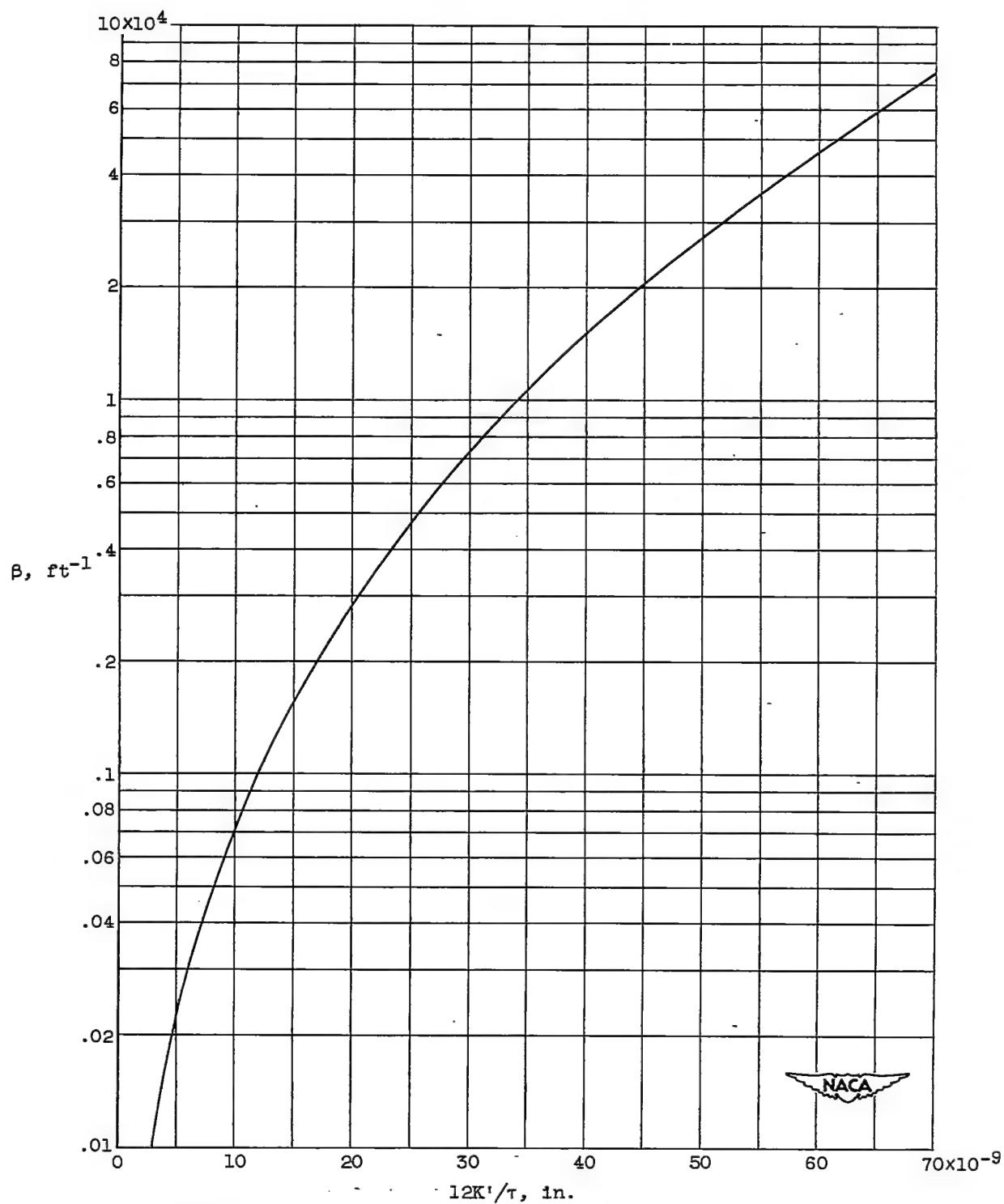


Figure 4. - Relation between factor  $\beta$  and permeability for curves used in analysis.

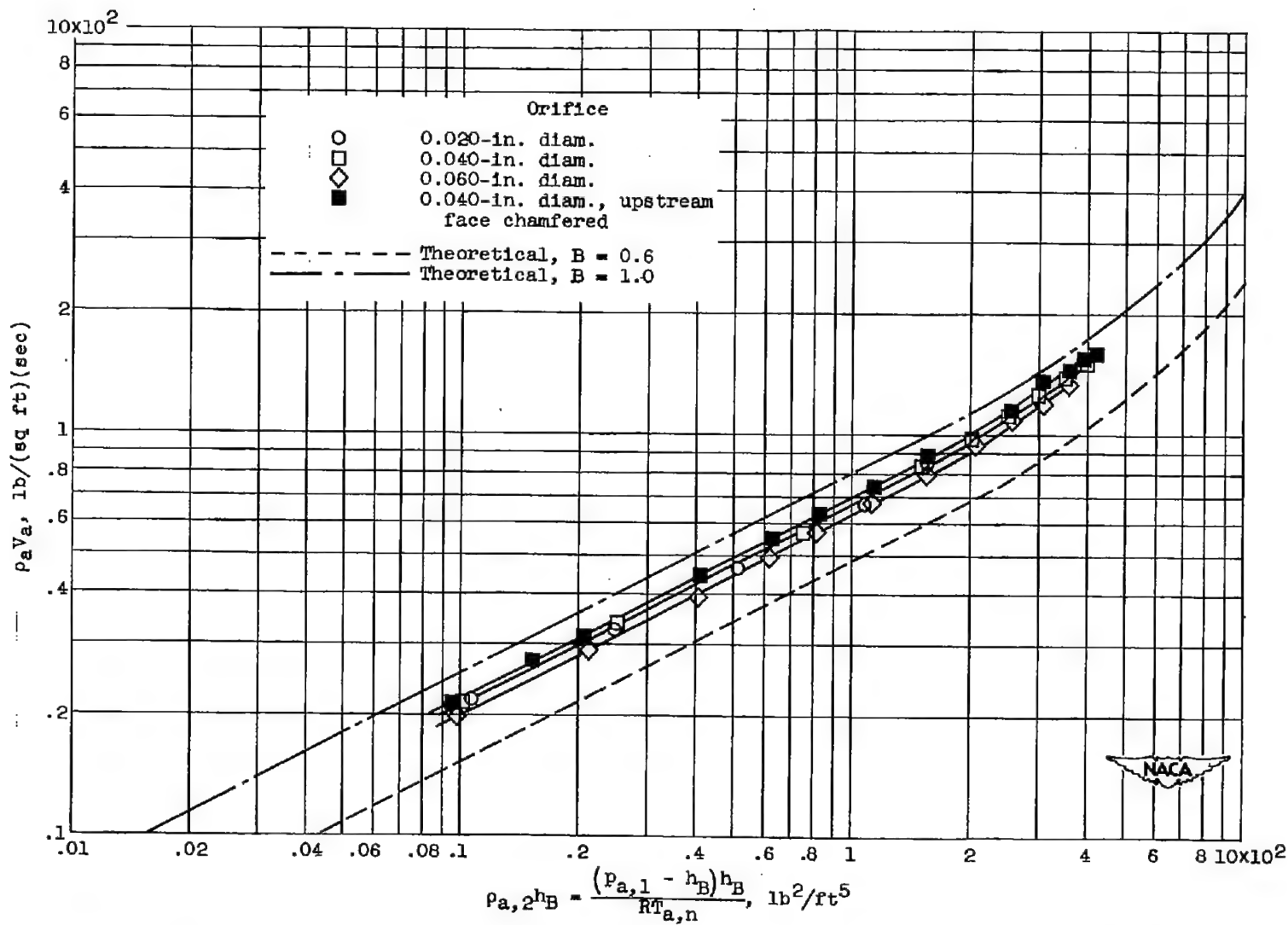
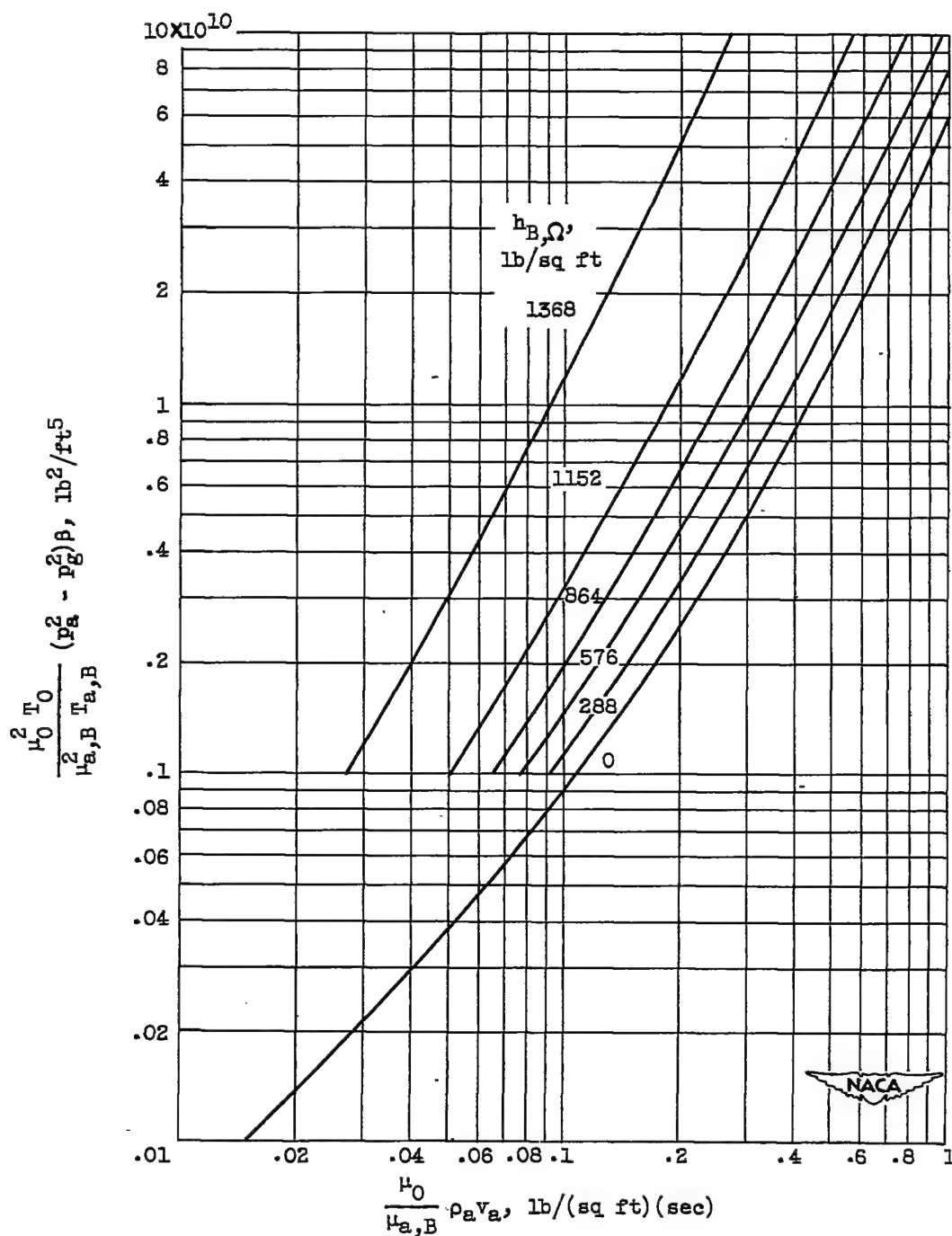
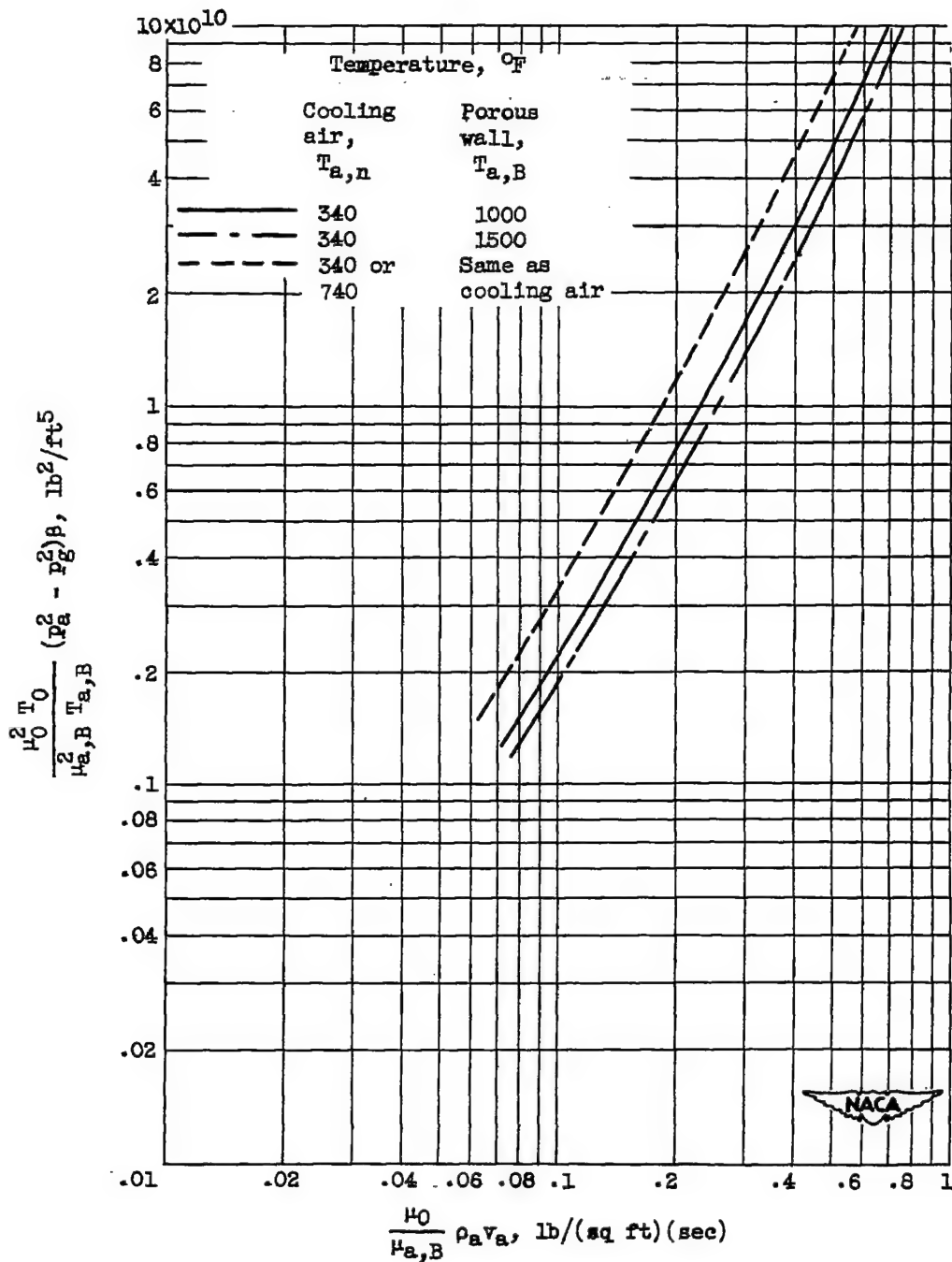


Figure 5. - Calibration of small-diameter orifices where orifice plate thickness is large compared with standard flat-plate orifice practice.



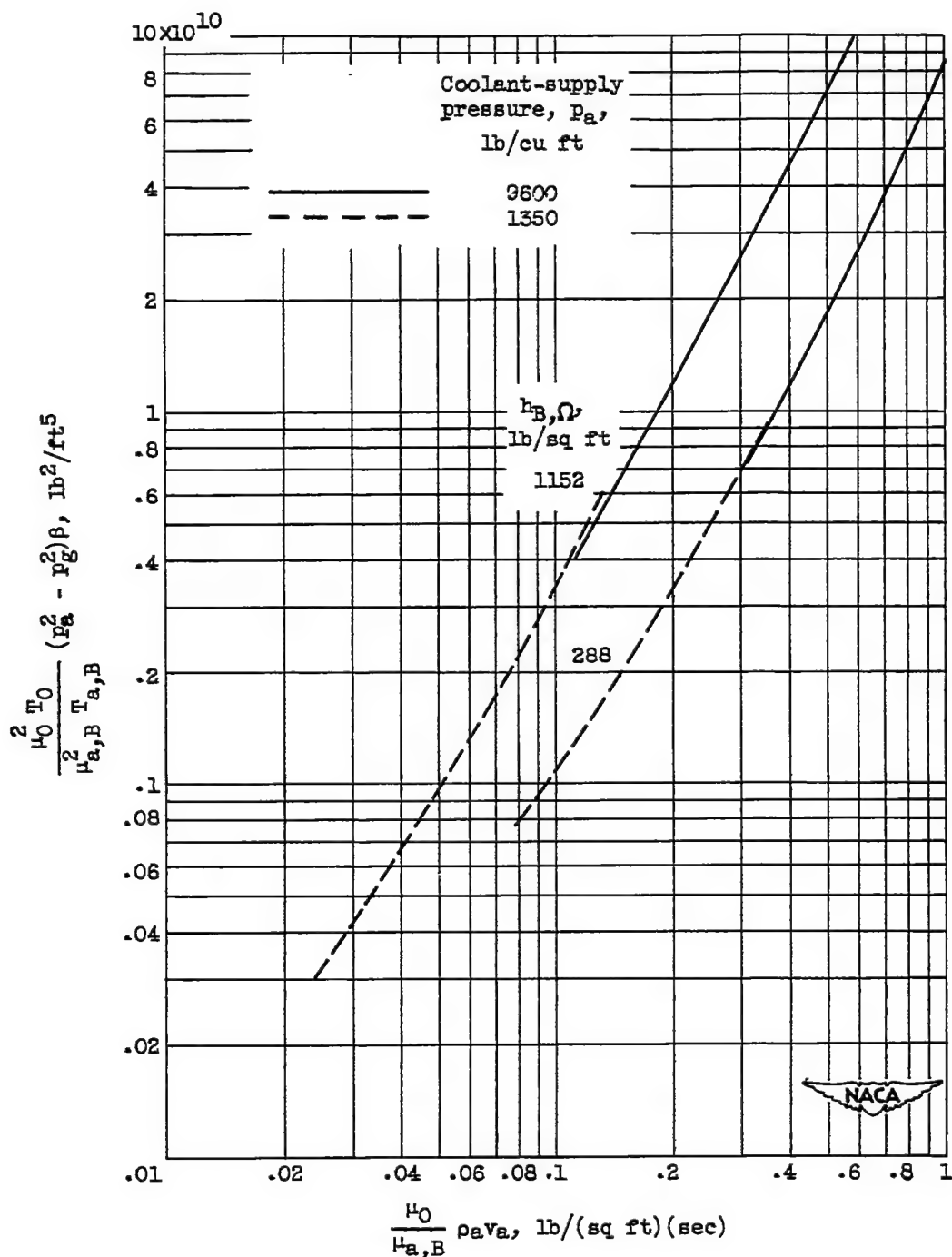
(a) Effect of orifice size. Permeability,  $40 \times 10^{-9}$  inch;  
coolant-supply pressure, 9600 pounds per square foot;  
cooling-air ( $T_{a,n}$ ) and porous-wall ( $T_{a,B}$ ) temperatures,  
740° F.

Figure 6. - Correlation of flow rates through porous surfaces  
in series with metering orifices.



(b) Effect of cooling-air and porous-wall temperatures. Permeability ( $12K'/\tau$ ),  $40 \times 10^{-9}$  inch; pressure drop  $h_{B,\Omega}$ , 1152 pounds per square foot; coolant-supply pressure, 9600 pounds per square foot.

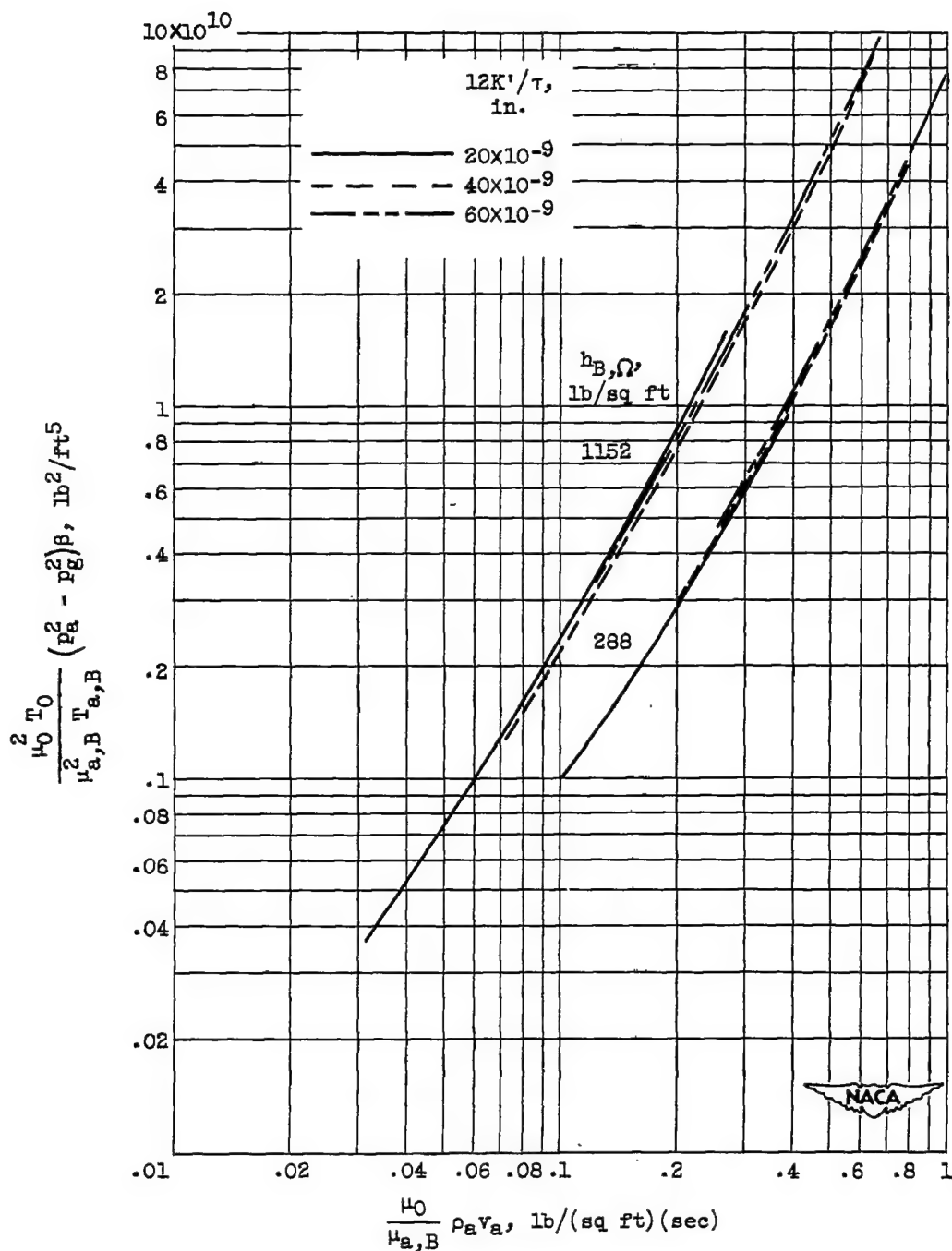
Figure 6. - Continued. Correlation of flow rates through porous surfaces in series with metering orifices.



(c) Effect of coolant-supply pressure for two orifice sizes. Permeability ( $12K'/\tau$ ),  $40 \times 10^{-9}$  inch; cooling-air ( $T_{a,n}$ ) and porous-wall ( $T_{a,B}$ ) temperatures,  $340^\circ$  F.

Figure 6. - Continued. Correlation of flow rates through porous surfaces in series with metering orifices.





(d) Effect of porous-material permeability for two orifice sizes. Coolant-supply pressure, 9600 pounds per square foot; cooling-air temperature ( $T_{a,n}$ ), 340° F; porous-wall temperature ( $T_{a,B}$ ), 1000° F.

Figure 6. - Concluded. Correlation of flow rates through porous surfaces in series with metering orifices.

2979

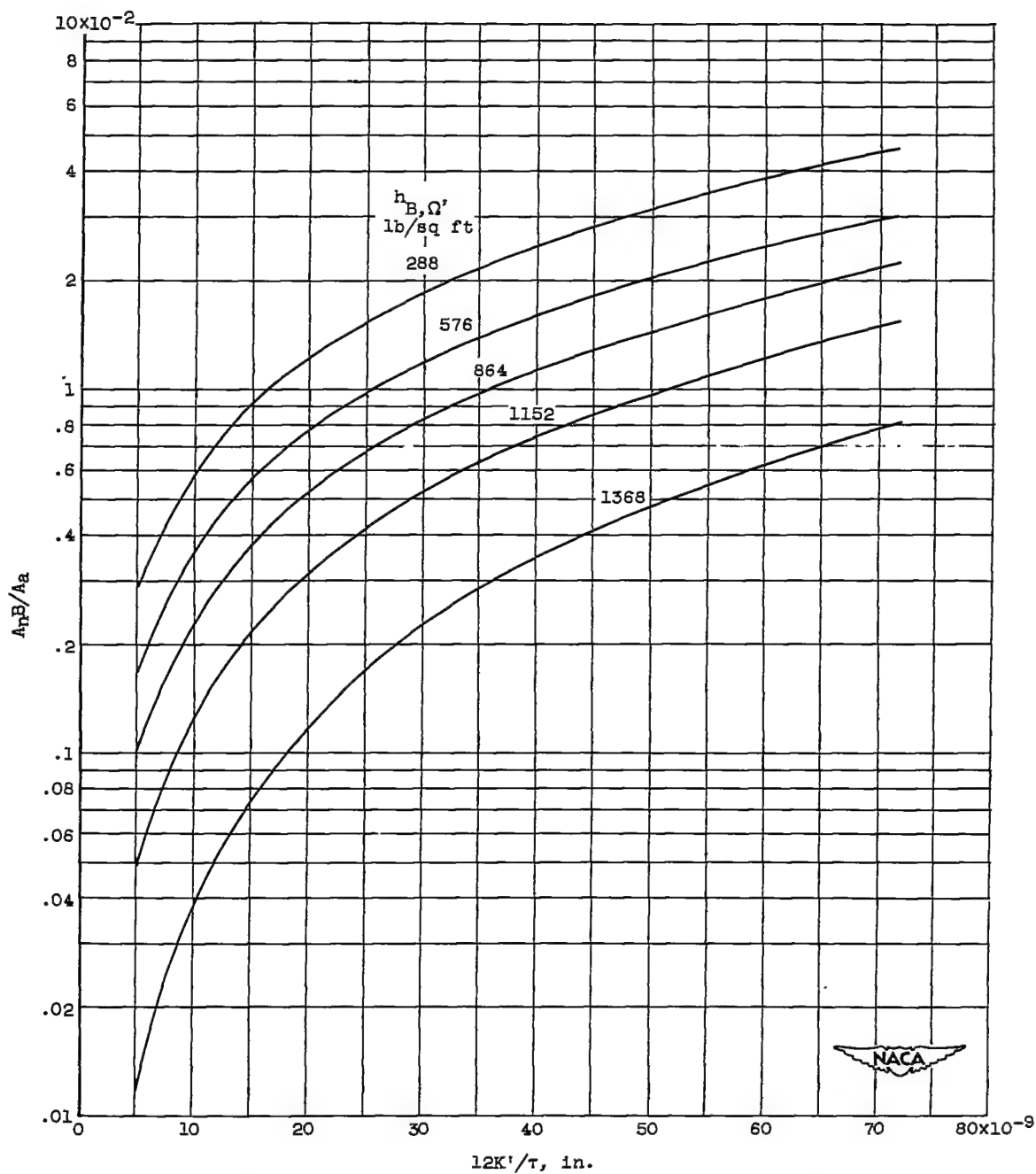
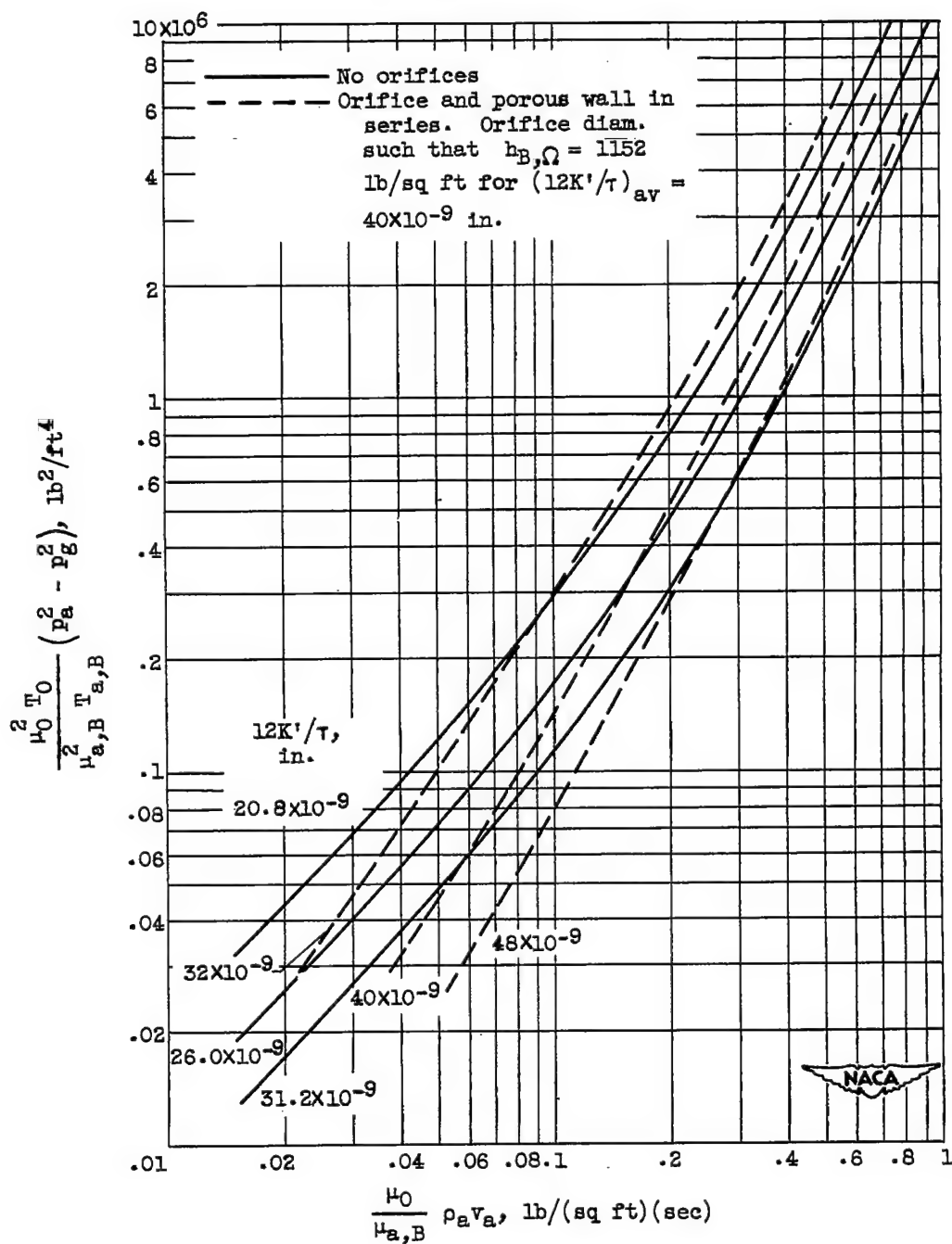
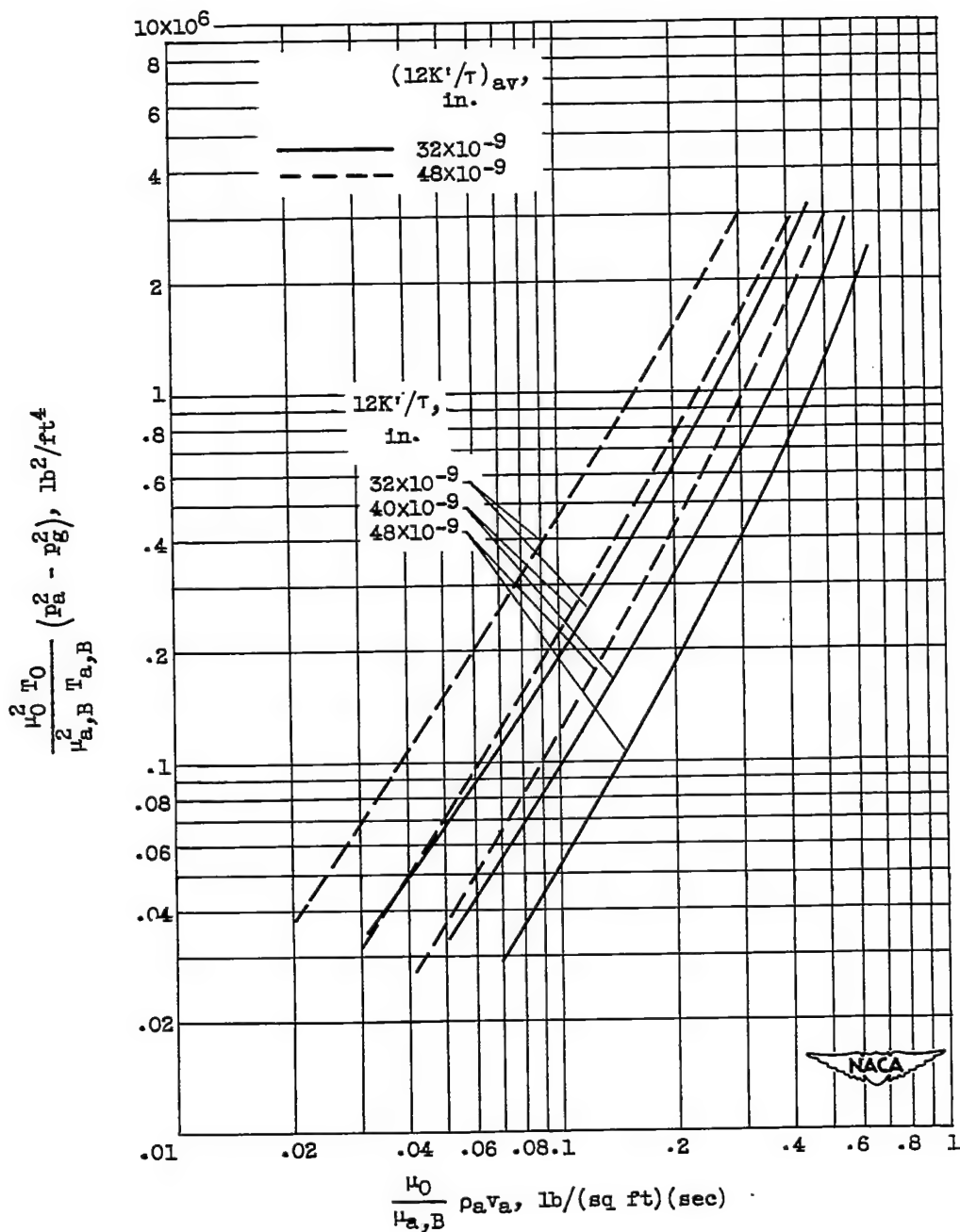


Figure 7. - Determination of orifice size for various orifice pressure drops and various porous-wall permeabilities.



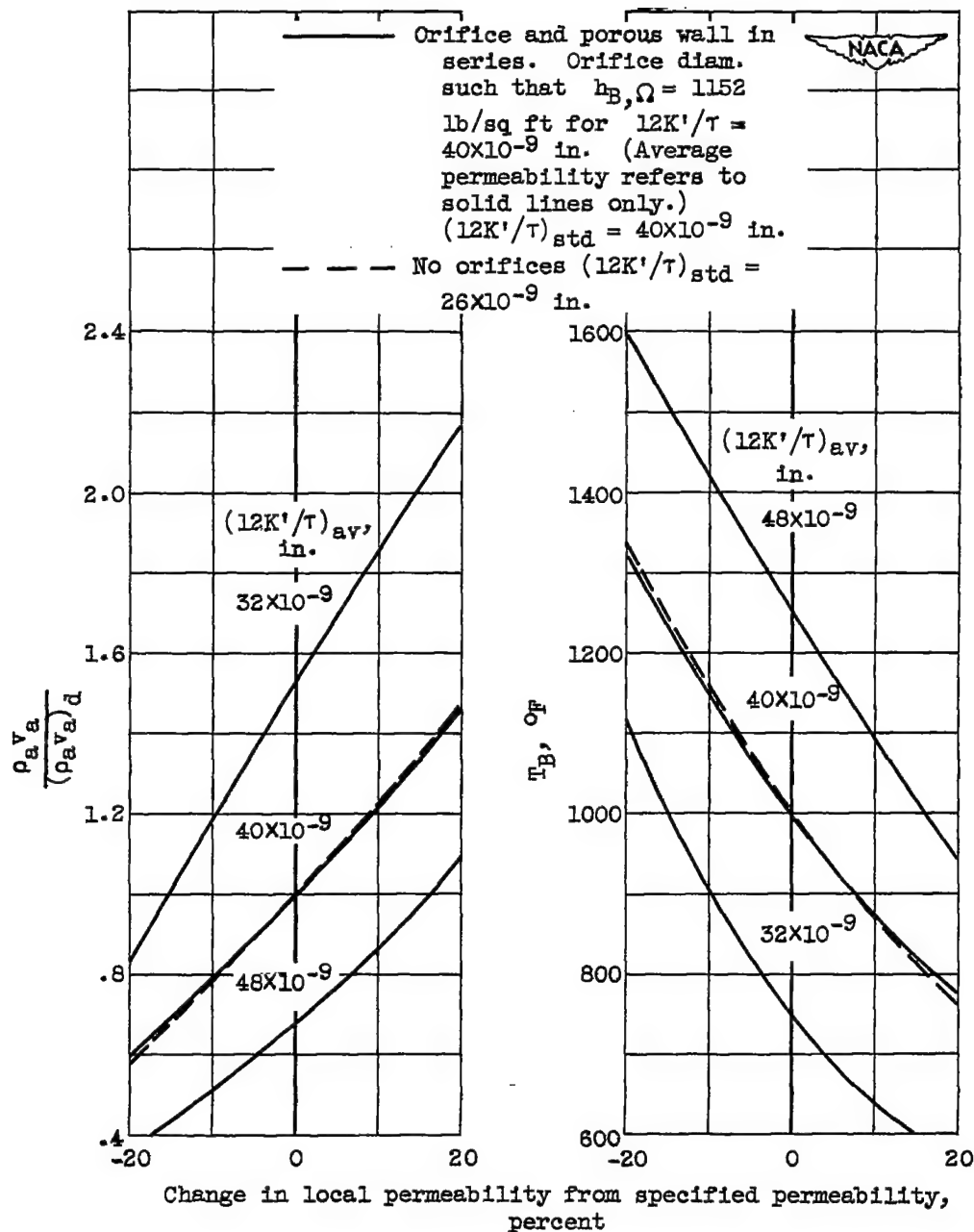
(a) Comparison of flow rates for porous materials with and without orifices in series.

Figure 8. - Effect of 20-percent variations in permeability of porous materials on coolant-flow rates. Coolant-supply pressure, 9600 pounds per square foot; cooling-air temperature, 340° F; porous-wall temperature, 1000° F.



(b) Effect of average permeability on local coolant-flow rates for porous materials in series with orifices. Orifice diameter such that  $h_{p,\Omega} = 1152$  pounds per square foot for average permeability  $(12K'/\tau)_{av}$  of  $40 \times 10^{-9}$  inch.

Figure 8. - Concluded. Effect of 20-percent variations in permeability of porous materials on coolant-flow rates. Coolant-supply pressure, 9600 pounds per square foot; cooling-air temperature,  $340^\circ \text{F}$ ; porous-wall temperature,  $1000^\circ \text{F}$ .

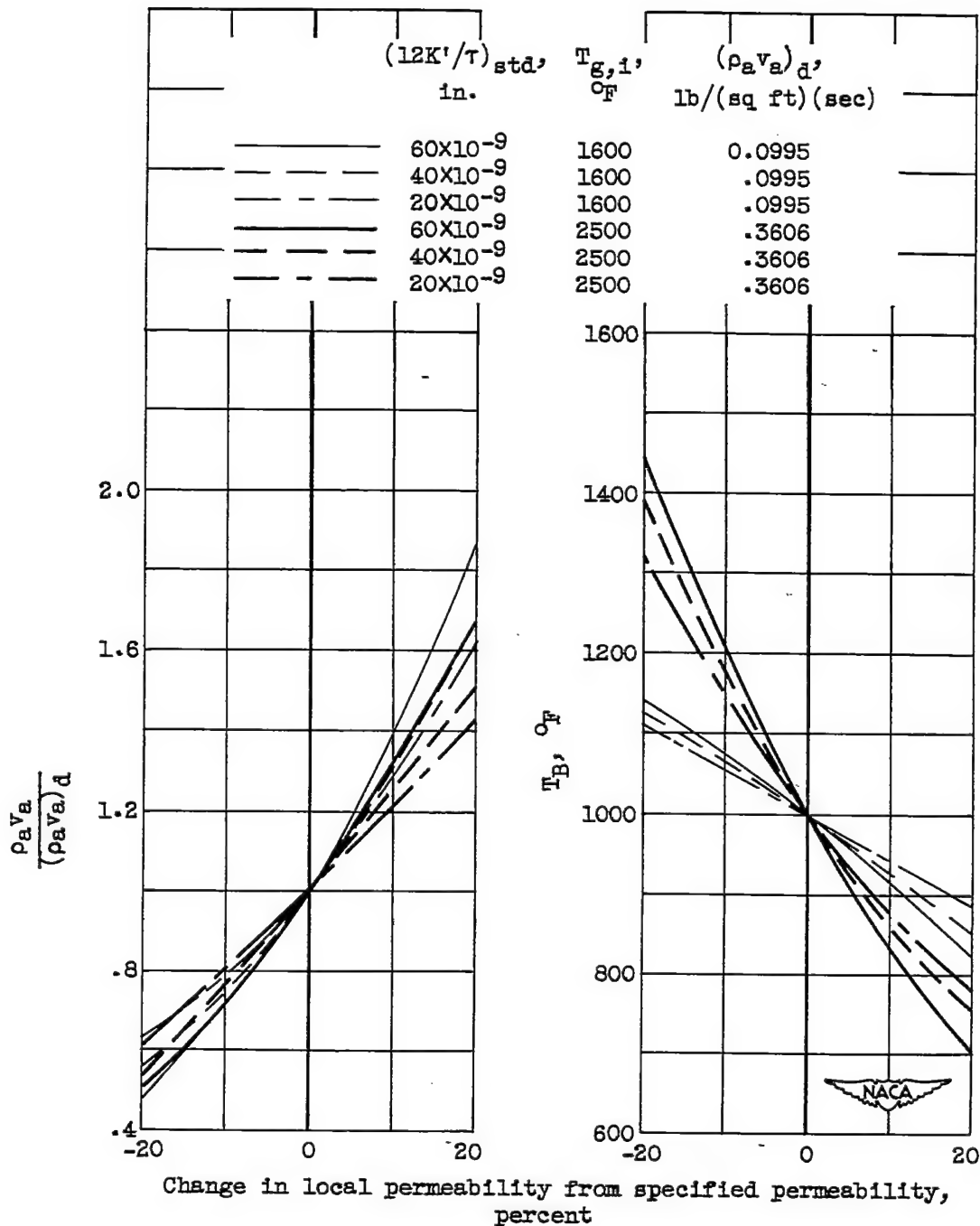


(a) Flow through orifices and porous surfaces in series for various average permeabilities and through an equivalent porous material without orifices. Coolant-supply pressure, 9600 pounds per square foot; turbine-inlet gas temperature, 2500° F; gas Reynolds number,  $2 \times 10^5$ ; design coolant flow, 0.361 lb/(sq ft)(sec).

Figure 9. - Effect of local permeability variations on blade temperature and coolant flow. Cooling-air temperature, 340° F.

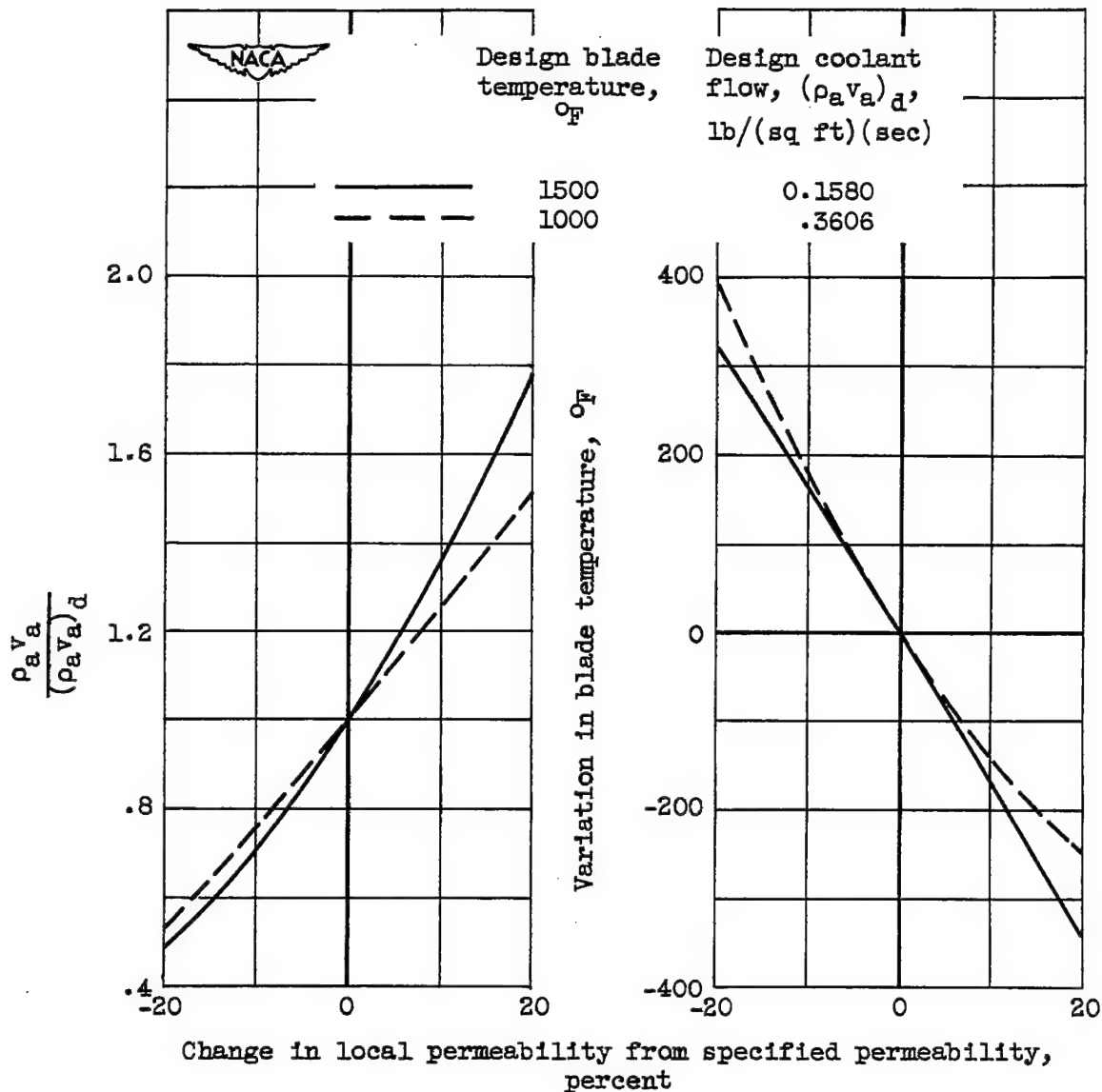
2979

CP-7 back



(b) Various magnitudes of specified permeability and two turbine-inlet temperatures. Gas Reynolds number,  $2 \times 10^5$ ; no orifices.

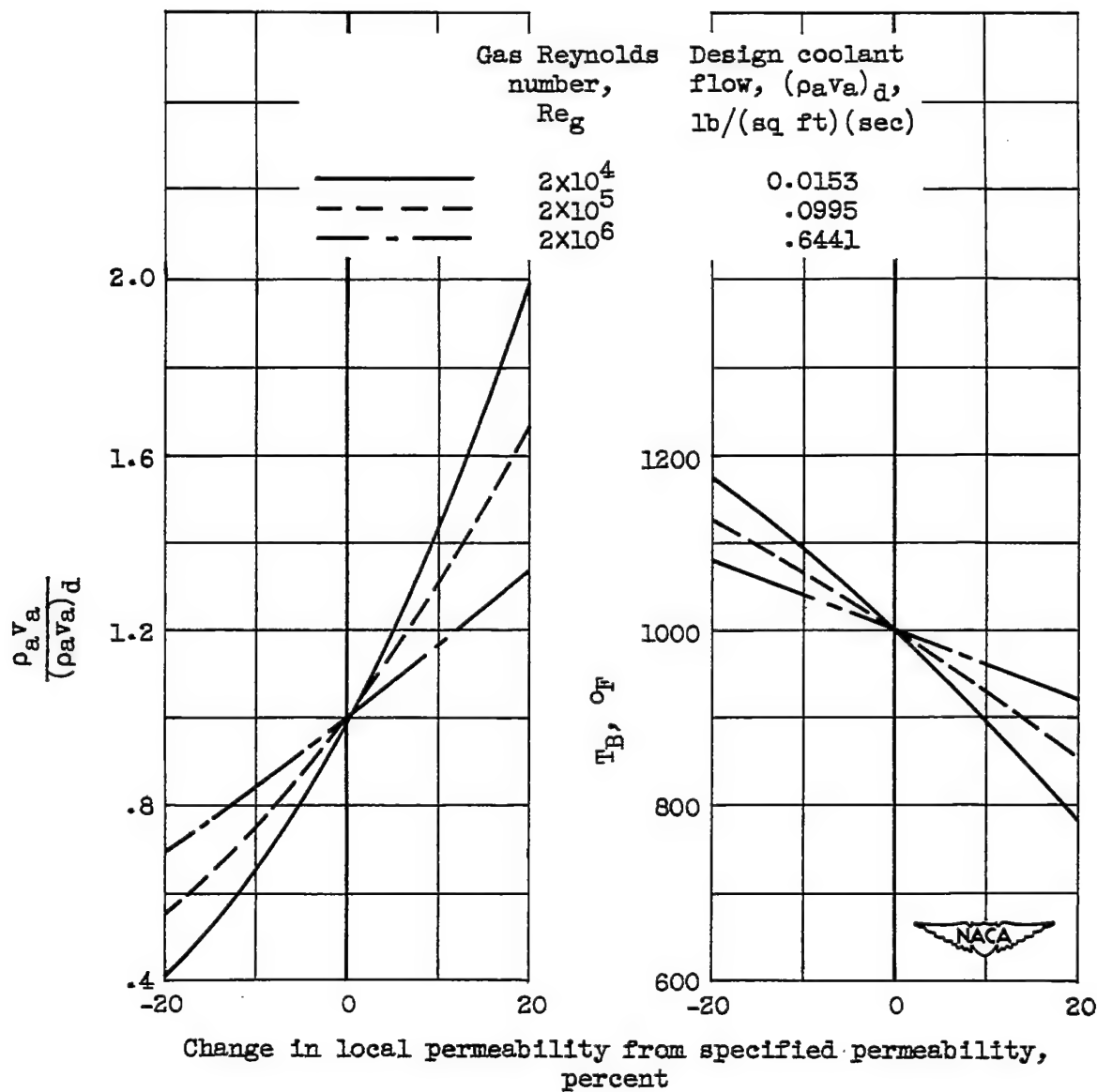
Figure 9. - Continued. Effect of local permeability variations on blade temperature and coolant flow. Cooling-air temperature,  $340^{\circ}F$ .



(c) Two design blade temperatures. Turbine-inlet gas temperature, 2500° F; gas Reynolds number,  $2 \times 10^5$ ; specified permeability,  $40 \times 10^{-9}$  inch; no orifices.

Figure 9. - Continued. Effect of local permeability variations on blade temperature and coolant flow. Cooling-air temperature, 340° F.





(d) Three gas Reynolds numbers. Turbine-inlet gas temperature, 1600° F; specified permeability,  $40 \times 10^{-9}$  inch; no orifices.

Figure 9. - Concluded. Effect of local permeability variations on blade temperature and coolant flow. Cooling-air temperature, 340° F.

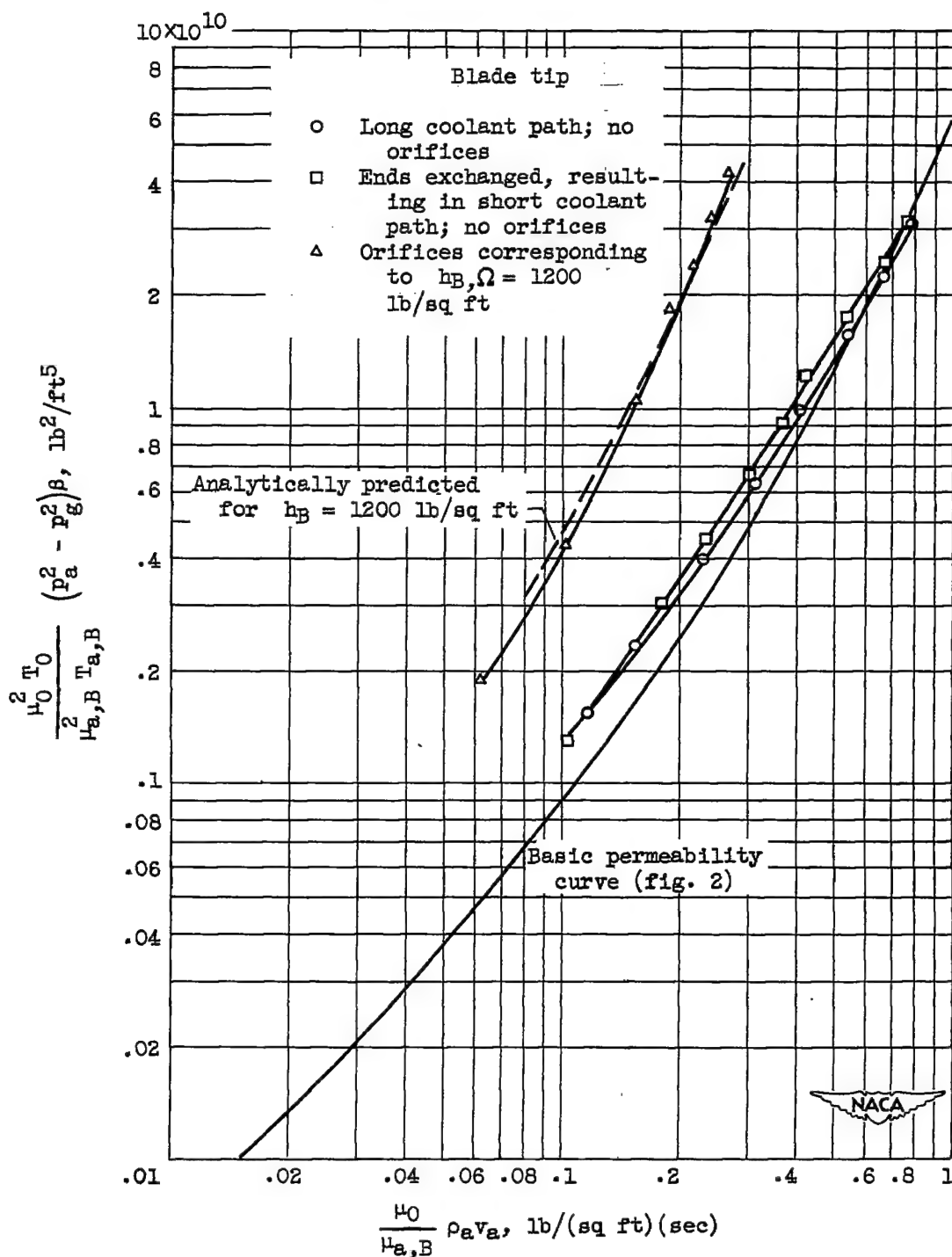


Figure 10. - Permeability correlation curves from experimental blade showing effects of coolant-passage pressure losses and orifices at blade base. Permeability ( $12K'/\tau$ ),  $18 \times 10^{-9}$  inch.

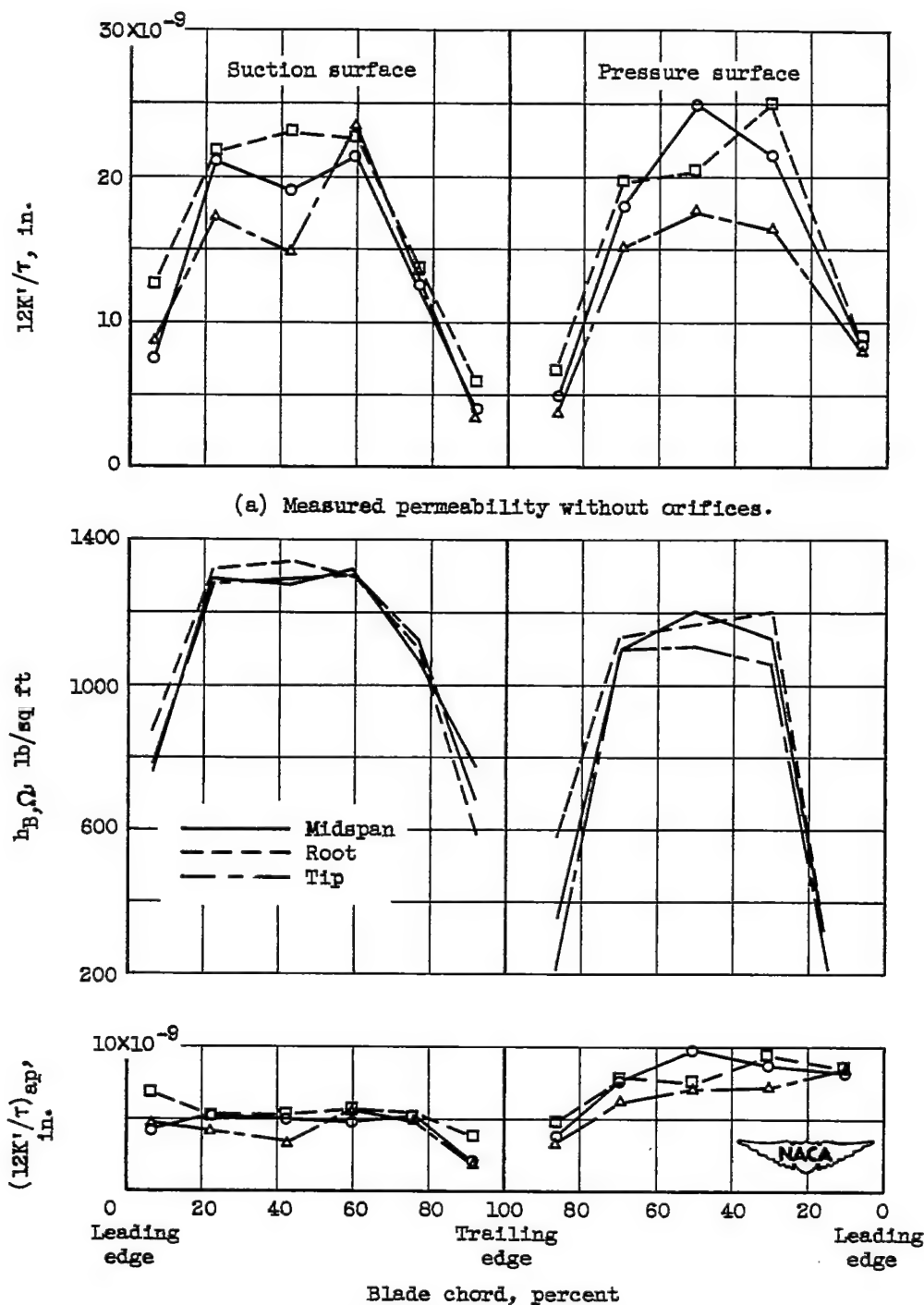
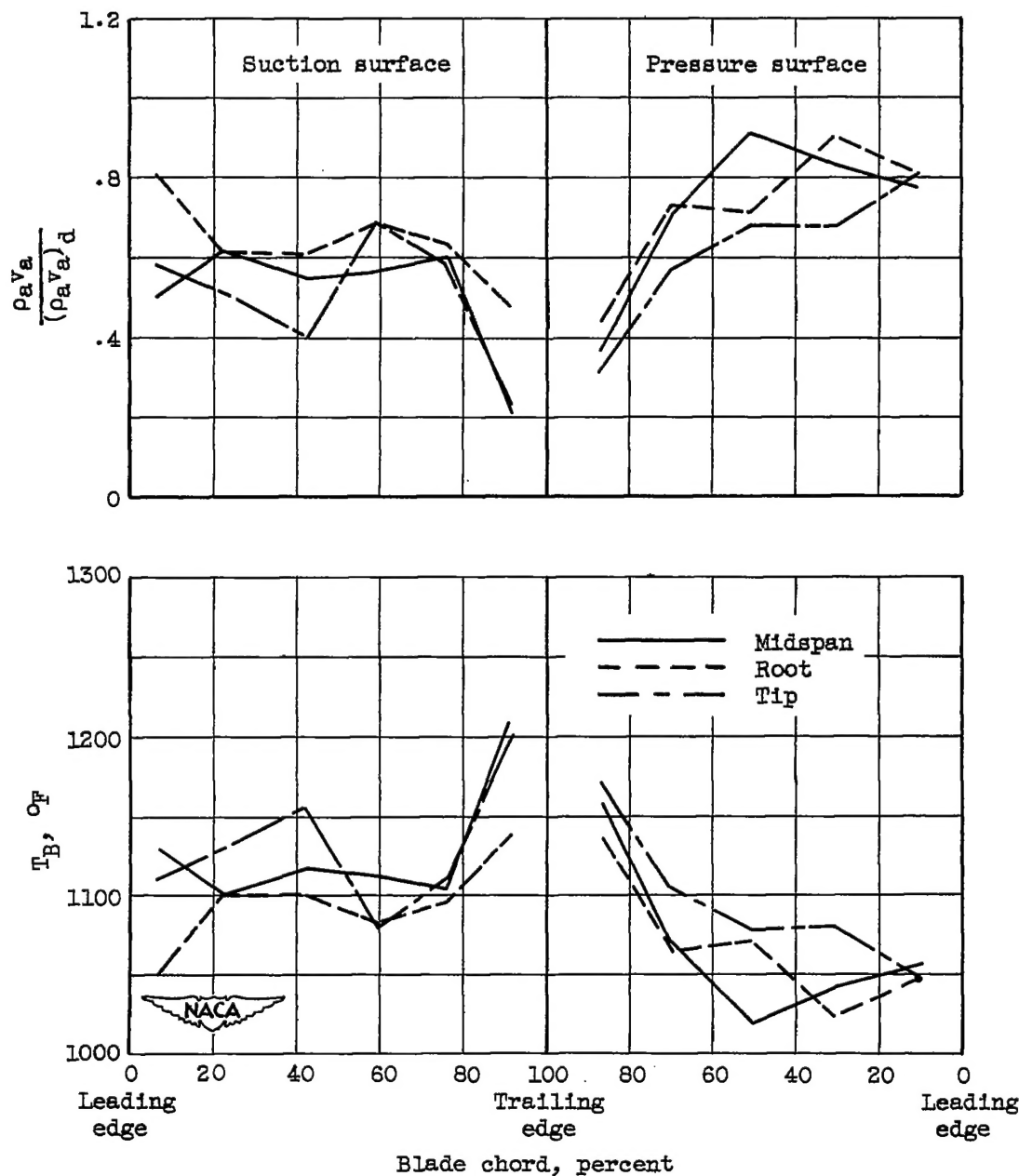
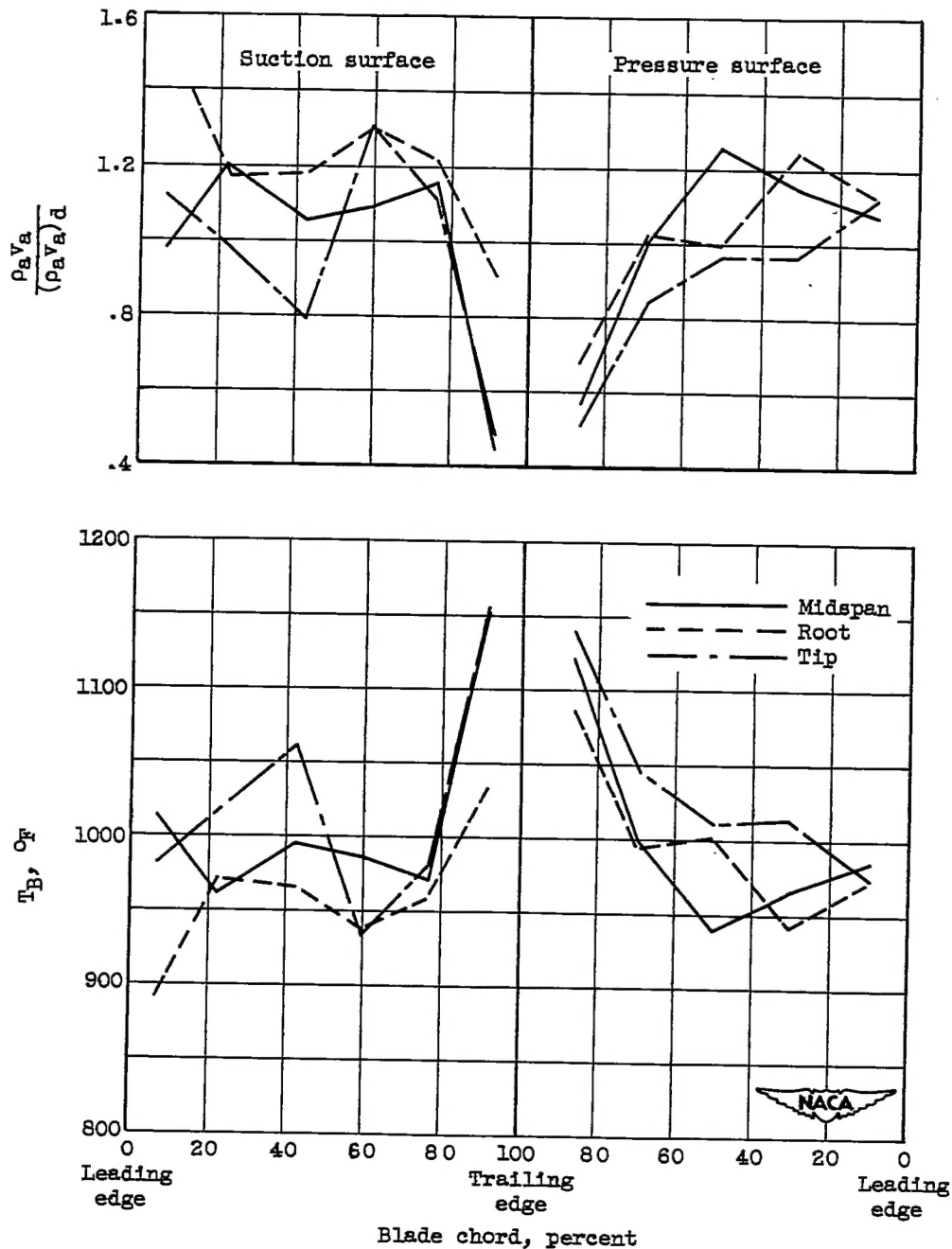


Figure 11. - Experimentally measured permeability distributions around periphery of experimental blade with and without orifices at blade base for three spanwise positions.



(a) Distribution based upon originally specified apparent permeabilities of  $8.7 \times 10^{-9}$  inch on suction surface and  $10.4 \times 10^{-9}$  inch on pressure surface.

Figure 12. - Effect of experimental blade permeability variations on blade-temperature and coolant-flow distributions for three spanwise positions on blade. Gas Reynolds number,  $5 \times 10^5$ ; gas temperature,  $1600^\circ \text{F}$ ; cooling-air temperature,  $340^\circ \text{F}$ .



(b) Distributions based upon average apparent permeabilities of  $4.5 \times 10^{-9}$  inch on suction surface and  $7.5 \times 10^{-9}$  inch on pressure surface.

Figure 12. - Concluded. Effect of experimental blade permeability variations on blade-temperature and coolant-flow distributions for three spanwise positions on blade. Gas Reynolds number,  $5 \times 10^5$ ; gas temperature,  $1600^\circ F$ ; cooling-air temperature,  $340^\circ F$ .

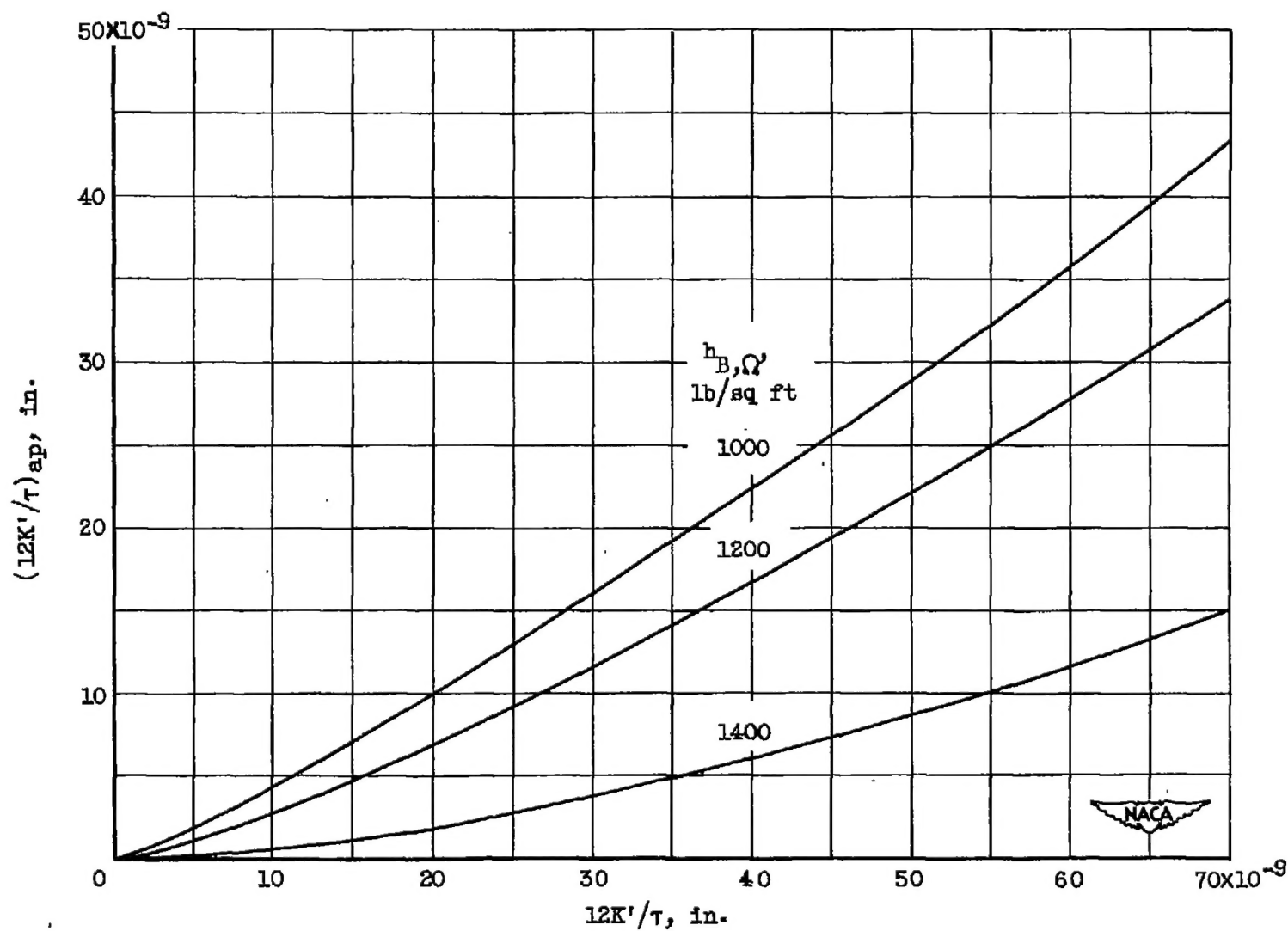
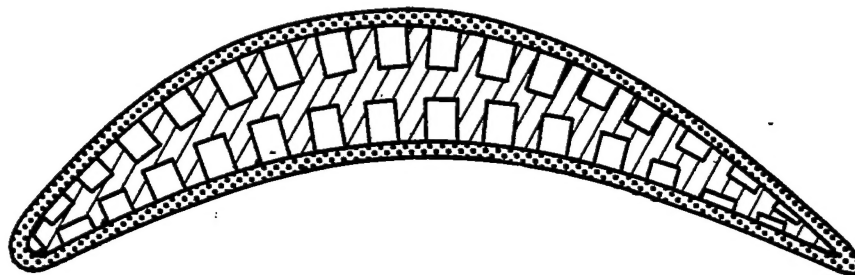
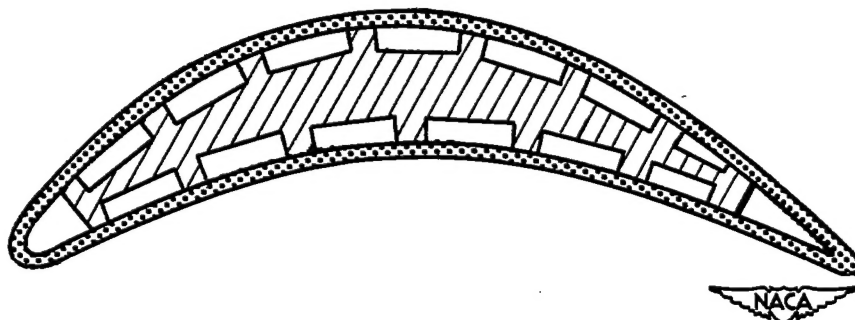


Figure 13. - Relation between apparent and actual permeability for range of  $h_{B,\Omega}$  recommended for gas-turbine blades.



(a) Strut configuration of experimental blade investigated.



(b) A proposed strut configuration.

Figure 14. - Sketches of two strut configurations for strut-supported, transpiration-cooled turbine blades.